



**US Army Corps
of Engineers®**
Engineer Research and
Development Center

ERDC/CRREL LR-04-16

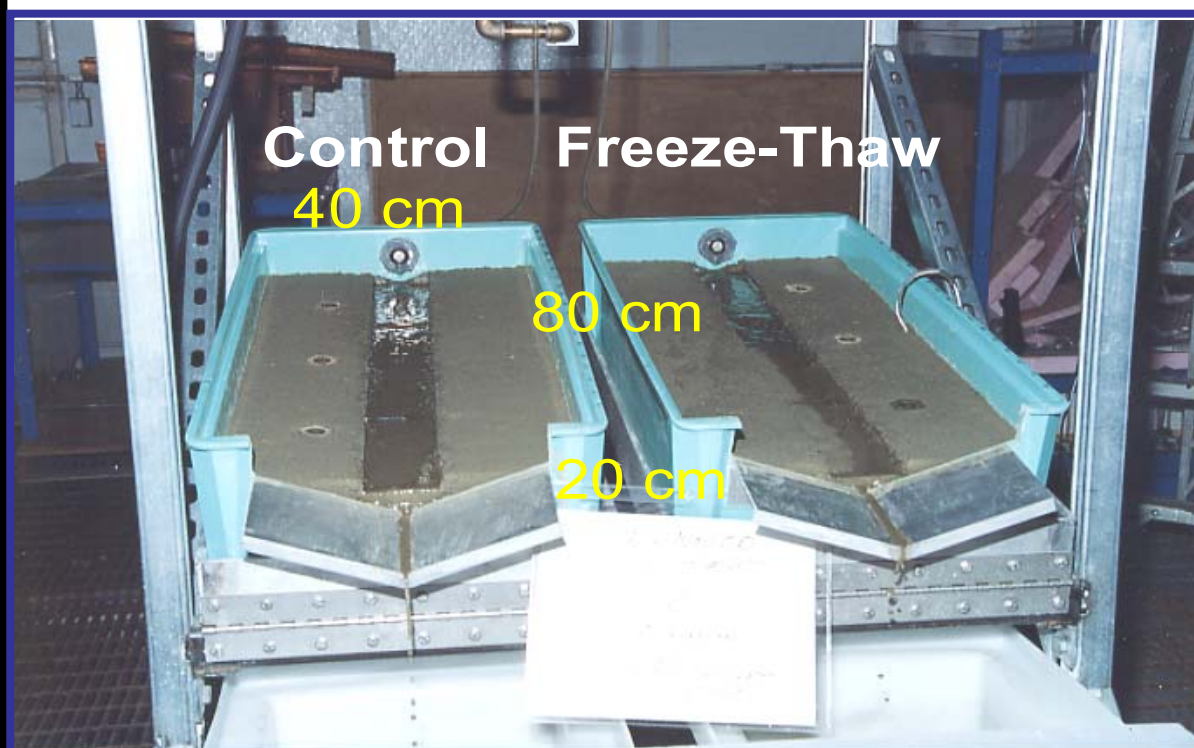
**Cold Regions Research
and Engineering Laboratory**

Quantifying the Effect of a Freeze–Thaw Cycle on Soil Erosion

Laboratory Experiments

M.G. Ferrick and L.W. Gatto

July 2004



Quantifying the Effect of a Freeze–Thaw Cycle on Soil Erosion: Laboratory Experiments

M.G. Ferrick and L.W. Gatto *

**Cold Regions Research and Engineering Laboratory
U.S. Army Engineer Research and Development Center
72 Lyme Road
Hanover, New Hampshire 03755*

ABSTRACT

In this paper we quantitatively tested the hypothesis that soil freeze–thaw (FT) processes significantly increase the potential for upland hillslope erosion during runoff events that follow thaw. We selected a frost-susceptible silt to obtain an upper bound on FT effects, and completed three series of six experiments each to quantify differences in soil erodibility and rill development for bare soil following a single FT cycle. Each series represented a specific soil moisture range: 16–18%, 27–30%, and 37–40% by volume, with nominal flow rates of 0.4, 1.2, and 2.4 L/min and slopes of 8° and 15°. Each experiment used two identical soil bins, one a control (C) to remain unfrozen, the other to be frozen and thawed. Standard soil characterization tests did not detect significant differences between the FT and C bins. Experimental results were closely related to conditions of the experiment, imposing a requirement for minimum differences in soil weight, bulk density, and soil moisture through each series. We measured cross-sectional geometry of an imposed straight rectangular rill before each experiment, sediment load during, and rill cross sections after. Changes in cross section provided detailed measures of erosion at specific locations along the rill, while sediment load from time series runoff samples integrated the rill erosion. Several parameters, including average maximum rill width, average maximum rill depth, rill cross-section depth measures, and sediment load all followed similar trends. Each was greater in the FT than in the C, with values that generally increased with slope and flow. However, soil moisture was the only parameter that affected the FT/C relationship. For example, average sediment load grouped by soil moisture provided FT/C ratios of 2.4, 3.0, and 5.0 for low, mid, and high moisture, respectively. In contrast, a “dry” experiment at 4.4% soil moisture had FT/C of 1.02 for sediment load. These results indicate a dramatic increase in the rate and quantity of bare soil eroded as a result of the FT cycle that is in direct proportion to soil moisture.

DISCLAIMER: The contents of this report are not to be used for advertising, publication, or promotional purposes. Citation of trade names does not constitute an official endorsement or approval of the use of such commercial products. All product names and trademarks cited are the property of their respective owners. The findings of this report are not to be construed as an official Department of the Army position unless so designated by other authorized documents.

Quantifying the Effect of a Freeze–Thaw Cycle on Soil Erosion: Laboratory Experiments

M.G. Ferrick and L.W. Gatto
Environmental Sciences Branch
Cold Regions Research and Engineering Laboratory
Engineer Research and Development Center
72 Lyme Rd.
Hanover, NH 03755-1290
Michael.G.Ferrick@erdc.usace.army.mil
Lawrence.W.Gatto@erdc.usace.army.mil

Abstract. In this paper we quantitatively tested the hypothesis that soil freeze–thaw (FT) processes significantly increase the potential for upland hillslope erosion during runoff events that follow thaw. We selected a frost-susceptible silt to obtain an upper bound on FT effects, and completed three series of six experiments each to quantify differences in soil erodibility and rill development for bare soil following a single FT cycle. Each series represented a specific soil moisture range: 16–18%, 27–30%, and 37–40% by volume, with nominal flow rates of 0.4, 1.2, and 2.4 L/min and slopes of 8° and 15°. Each experiment used two identical soil bins, one a control (C) to remain unfrozen, the other to be frozen and thawed. Standard soil characterization tests did not detect significant differences between the FT and C bins. Experimental results were closely related to conditions of the experiment, imposing a requirement for minimum differences in soil weight, bulk density, and soil moisture through each series. We measured cross-sectional geometry of an imposed straight rectangular rill before each experiment, sediment load during, and rill cross sections after. Changes in cross section provided detailed measures of erosion at specific locations along the rill, while sediment load from time series runoff samples integrated the rill erosion. Several parameters, including average maximum rill width, average maximum rill depth, rill cross-section depth measures, and sediment load all followed similar trends. Each was greater in the FT than in the C, with values that generally increased with slope and flow. However, soil moisture was the only parameter that affected the FT/C relationship. For example, average sediment load grouped by soil moisture provided FT/C ratios of 2.4, 3.0, and 5.0 for low, mid, and high moisture, respectively. In contrast, a “dry” experiment at 4.4% soil moisture had FT/C of 1.02 for sediment load. These results indicate a dramatic increase in the rate and quantity of bare soil eroded as a result of the FT cycle that is in direct proportion to soil moisture.

Keywords: Soil erosion, rill development, freeze–thaw effects, overland flow

Introduction

Soil is eroded as surface water flows over bare or partially vegetated hillslopes. The quantities and rates of erosion depend on the resistance of soil particles to detachment and the transport capacity of the runoff. Soil particle detachment varies with inter-particle friction, bonding, and interlocking, and the sediment transport capacity of runoff is a function of velocity and turbulence. The capability of a soil to resist erosion depends on soil-particle size and distribution, soil structure and structural stability, soil permeability, water content, organic content, and mineral and chemical constituents (Lal and Elliot, 1994). Low-density soils are more readily eroded, while compaction generally increases erosion resistance. Because of significant seasonal changes in both soil density and moisture, Pall et al. (1982) proposed erodibility as a time-varying rather than static soil characteristic. Thus, a combination of many factors determines the volume of sediment eroded during a runoff event. Because of this complexity, coefficients of the rill erosion equation used in the WEPP model have been found to vary by one to two orders of magnitude (Elliot et al., 1990).

During periods of decreasing air temperature, heat is lost from the soil surface. When sufficient heat is lost, water in the soil begins to freeze. The net effect of this ice formation on soil structure depends on soil type, water content, and intensity of the freezing. Freezing and thawing of soils cause movement of water and solutes in the profile (Radke and Berry, 1997; Gatto, 2000). Water can move upward toward the freezing front, allowing ice lenses or layers to form. Three conditions must exist for ground ice to grow and become a substantial component of a soil mass: an adequate supply of soil moisture, sufficiently cold air temperatures to cause heat loss and freezing, and a frost-susceptible soil with a significant silt component (Anderson et al., 1978). Silts absorb water rapidly because the particles are small enough to provide high capillary rise and yet large enough so that pore spaces allow quick flow of water through the soil (Jumikis, 1962). These characteristics promote a rapid increase in moisture content within the pores near the location of freezing. Water movement through more fine-grained soils is much slower, and coarse-grained soils do not develop sufficient capillary forces to move soil moisture to the freezing front. Thus, silts with available soil water are most susceptible to the changes in strength and erodibility caused by FT cycling. However, Janson (1963) reports that even sand may become frost susceptible if it is well compacted, and Chamberlain (personal communication) has observed needle ice in almost any soil type. In addition to soil texture, frost susceptibility depends upon vegetative cover; the thickness and density of snow cover; initial soil temperature and temperature gradient; air temperature regime; exposure to the sun; depth to the water table; overburden stress; and soil density (Jumikis, 1962; Chamberlain, 1981). As ice crystals form within soil voids particles are forced apart, and ice pressure may compress or rupture soil aggregates. These FT-induced, physical changes affect soil-particle cohesion, density and strength, surface soil moisture, infiltration capacity, runoff production, and soil-surface geometry, which, in turn, affect soil erodibility and the erosivity of subsequent runoff.

Benoit and Voorhees (1990) and Kok and McCool (1990) report that soil FT effects are some of the least understood aspects of soil erosion processes. Several investigators have recognized that FT generally increases soil erodibility (Bryan, 2000), and that the magnitude of this effect varies with soil texture, moisture, and extent of freezing. Laboratory experiments of Formanek et al. (1984) found that the shear strength of a silt loam was reduced to less than half its original value after one FT cycle, but

second and third cycles resulted in little additional reduction. Van Klaveren (1987) suggested that critical shear strength of soil might be half of its initial value after one FT cycle. Edwards and Burney (1987) used a laboratory rainfall simulator to determine that FT of a bare soil increased sediment loss by 90%, and that this loss increased significantly when overland flow was added. Rill erosion laboratory experiments of Van Klaveren and McCool (1998) revealed slightly higher erodibility of thawed soils after a single FT cycle compared to that of an unfrozen soil. Edwards et al. (1995) conducted similar laboratory tests, except that four diurnal cycles of freeze–thaw were performed prior to a final 12-hr freezing cycle. Erosion of this cycled and initially frozen soil produced a mean sediment yield 25% greater than a similar soil that had never been frozen. This overview of work to date suggests that the effects of FT on soil erosion vary, and that a quantitative parametric understanding does not yet exist.

The objective of the experiments described and analyzed in this paper was to isolate and quantify the effects of FT on soil erosion and rill development in bare soil. Frost-susceptible silt was used in the experiments to obtain an upper bound on the effects caused by a single FT cycle. Two identical soil bins were prepared for each experiment, one to remain unfrozen as a control (C), the other to be completely frozen and thawed (FT). This parallel approach allowed measured differences in soil loss to be directly attributed to the FT process and related to the other controlled parameters. Three series of experiments were performed, each within a specific soil moisture range. Each series included six experiments at three nominal flow rates and two slopes. Soil characterization for each soil moisture condition measured physical changes induced by FT. The results of the experiments were closely related to experimental conditions, imposing a need for tightly regulated soil moisture, bulk density, applied flow, and slope throughout each series. We performed replications of several experiments with differing variability in conditions to quantify the probable uncertainty and reliability of results.

Description of Experiments

We used frost-susceptible Hanover silt for all experiments to obtain an upper bound for FT effects on soil structure and subsequent overland-flow-induced erosion. Hanover silt is a low-plasticity, inorganic, clayey-silt classified as ML in the Unified Soil Classification System, with a specific gravity of 2.72, and a liquid limit of 28% (Shoop and Gatto, 1992). This soil is composed of 82% silt- and clay-sized particles by weight and 18% fine sand, with about 66% in the grain size range from 0.1 to 0.01 mm. During soil preparation the water content was adjusted into the appropriate range and periodically checked using either a Vitel Hydra or a Delta-T Theta probe. A resistivity sensor and thermistor were secured to the bottom of the FT bin prior to adding soil, and used to monitor the frozen or thawed state of the soil bottom. The FT and C bins were prepared with equal soil density by adding increments of equal weight that were compacted to the same thickness until a volume of about 38 L (79 cm long, 37 cm wide, 13 cm deep) was filled. Three groundwater wells were placed along one side of the longitudinal centerline of each bin, and the finished soil surface was flush with the tops of these wells. A metal plate, 8 cm wide by 1.5 cm thick, was tamped its full thickness into the soil between the flow inlet and the invert of the downstream weir. This imposed rectangular rill, with a compacted soil bottom, was oriented along the longitudinal centerline.

Prior to each experiment the FT bin was encased with 5-cm-thick insulation board and a freeze plate was placed on the soil surface to initiate freezing from the top, as in nature. The FT bin was frozen once to its full depth, and then thawed. Both the C and FT bins were sealed to minimize changes in soil moisture while the FT cycle progressed. The FT and C bins were then placed side-by-side in the CRREL soil-erosion simulator and elevated to the same slope. Equal incoming tap-water flows dropped about 3 cm from the flow inlet to the rill surface of each bin, flowed down the rills, and exited the bins via broad V-shaped weirs. At the start of each experiment the applied overland flow distributed uniformly across the width of these initial rills. The experimental setup is pictured in Figure 1.

Experiments were conducted in three series, each having a specific soil moisture range, 16–18% (low), 27–30% (mid), or 37–40% (high, saturated) by volume. Each series included six experiments at three nominal flow rates: 0.4, 1.2, and 2.4 L/min, and two slopes, 8° and 15°. The soil weight (kg) and pretest soil moisture (% by volume) of each bin are given in Table 1 by test series as mean \pm standard deviation. Comparisons between FT and C bin data reveal similar means and standard deviations for all series, with soil weight and moisture content increasing together, reflected in the mean bulk densities of each series. Freezing times given in Table 1 increased significantly with soil moisture because of the greater heat content. Thaw times were typically just over 24 hours.

We measured many parameters prior to, during, and following each experiment to quantify the erosion occurring in each bin. Included in these measurements were the cross-sectional geometry of the imposed rectangular rill at two locations before an experiment, sediment losses and flow discharge through time during, and eroded rill cross sections after. Sediment load gave an integrated measure of erosion through time, while cross-sectional data provided measures of erosion at specific locations. Both types of data were obtained to provide independent evidence, allowing us to assess the concurrence of trends, and yielding a stronger basis for conclusions. We measured rill cross sections and maximum rill widths and depths using a sliding pin meter to obtain horizontal distance from the bin wall and depth from the bin top to each point. Enough points were measured to adequately define rill cross-sectional shape. Figure 2 gives sample pre- and post-experiment cross sections for both bins. Maximum rill widths and depths were acquired at nine longitudinal locations spaced 0.1 of the bin length L apart.

We measured sediment losses and flow discharge by collecting timed samples throughout the experiment. Samples of 250 mL were collected at 1, 2, 3, 5, 7, and 10 minutes from the start of an experiment, and 500-mL samples followed at 12, 15, 20, and every 5 minutes thereafter until the end of the experiment. The sampling intervals increased as the experiment progressed and the rate of erosion generally slowed. The fill times of the known volume provided discharge measurements, and filtered samples quantified total sediment in transport. We used a cm-rule scaled in 10ths of a cm to measure groundwater depths in each well before, many times during, and again after each experiment. Pins were inserted at nine locations spaced along the rill to mark the waterline at the end of each experiment. We then measured the location and elevation of each pin, and calculated the overall water surface slope. During each experiment we visually observed and described the FT and C rill channels as they developed, and recorded these observations. In addition, photographs documented rill development at a two-minute interval from a position 1.6 m directly above the bins.

Soil Characterization

Special soil bins were prepared for each soil moisture series, and characterization measurements were obtained both to verify similarity between C and FT soils prior to freezing and quantify differences after the FT cycle. Penetration resistance was measured with an ELE International Proctor Penetrometer, and these pre-freeze compressive strengths were essentially identical in each bin, both within and outside the rill. Additional post-thaw measurements included in-rill and out-of-rill shear strength with a Pilcon handheld vane tester, and constant head infiltration time with a 5-cm-interior-diameter cylindrical infiltrometer. We calculated porosity, % soil water by volume, % saturation, and moist and dry unit weights of soil cores taken with an Eley volumeter. The post-thaw data are summarized in Tables 2, 3, and 4 for the low, mid, and high soil moisture conditions, respectively. In-rill penetrometer compressive strengths were higher than those outside the rill at low soil moisture, but this difference diminished for wetter soils. Mid-moisture compressive strengths were highest, decreasing at both lower and higher soil moistures. Reductions in compressive strength due to FT were either minor or negligible. Both the magnitude of and the difference between in-rill and out-of-rill vane shear measurements peaked at the lowest soil moisture and diminished as moisture increased. Vane shear strength measurements following FT were, at most, slightly reduced relative to the controls. Contrary to the results of Formanek et al. (1984) and Van Klaveren (1987), neither the penetrometer nor the vane shear data indicated a significant effect of FT on soil strength.

Infiltration rates diminished significantly with increasing soil moisture over the range of these experiments. At low moisture the infiltration rates outside the rill were much greater than those in the rill, and FT produced an even larger increase in all the rates. Mid soil moisture infiltrations were all significantly slower, but relatively rapid rates were more frequently found outside the rill. The value in parentheses following >3600 (Table 3) indicates the number of very slow infiltration results. At mid moisture the FT bin infiltration was not more rapid than that in the C bin. At high soil moisture all infiltrations were negligible. Infiltration into Hanover silt diminished significantly as soil moisture approached a saturated condition.

Cores taken in each bin from within and outside the rill completed our soil characterizations. With the exception of high soil moisture, the porosity in the rills was slightly less than that outside. Porosity diminished significantly between the low and mid moisture bins, and then was unchanged at high moisture. There was no measurable porosity difference between the FT and C bins at any soil moisture. Soil moisture data from the cores were largely in agreement with the probe measurements. Differences in soil moisture inside and outside the rills were not evident. Near-surface soil moisture in the FT bins after thaw was generally higher than that of the C bins, though differences diminished at high soil moisture. The saturation data largely follow the same trends as the soil moistures. The moist and dry unit weights in the rills are greater than those outside at low and mid soil moisture. However, this difference diminishes with increasing soil moisture, and is not evident at high moisture. Unit weights increase between the low and mid moisture bins, and then stay the same or decrease slightly at high soil moisture. There were no significant differences in the unit weights between the FT and C bins at any soil moisture.

Our conclusion is that this standard suite of bulk soil characterization measurements does not detect significant FT-induced changes in conditions between a soil that has been frozen and thawed, and the same soil that had not been frozen. This conclusion holds particularly well for saturated soil where the most pronounced effects of FT on flow-induced erosion are expected. The implication is that important changes caused by FT to enhance runoff-induced erosion following thaw occur at smaller scales approaching that of a pore, and measurements must sample these scales to be definitive.

Results

Overview

Rill development occurred with a repeatable progression through each experiment (Fig. 3), starting as a shallow, uniform sheet flow across the entire width of the imposed rill. In the early stages channels gradually developed near the edges of the imposed rectangular rill. The time required for an eroded channel to be discernible in the FT bin averaged over 10 minutes in the low-moisture series, 6 minutes in the mid-moisture series, and less than 3 minutes in the high-moisture series. Not all experiments developed a channel in the C bin, but for those that did, the overall average time was 21 minutes, a time that did not vary with soil moisture. These initially small channels typically grew in size and persisted for several minutes until one became the primary channel. This channel continued to enlarge and progressively captured the entire flow. The average time for a primary channel to develop along the entire length of the bin was 17.5 minutes in the FT, and when it developed, 34 minutes in the C. By experimental series average times in the FT decreased significantly as soil moisture increased, while the C average times also showed some decrease with increasing moisture. These data suggest that the FT soil was generally more erodible than that of the C, and this difference increased with soil moisture.

On average three–four knick points formed along the FT channel in all the moisture series, while three formed in the C during the low-moisture series and one or no knick points formed in the C channel during the mid- and high-moisture series. More significant channel development and deepening followed, primarily via knickpoint growth and upstream migration. While erosion progressed, the rills developed large-scale roughness and exhibited undercutting and sidewall sloughing, processes commonly observed in larger hillslope-scale rills. Experiments were terminated when erosion in the FT bin resulted in a deep rill over the entire channel length that reduced the final overall slope relative to the original applied slope. Erosion in the C bin frequently did not complete this rill development progression prior to termination of the experiment.

Duration (min), pre-experiment soil moisture content, and post-experiment water surface slope in each bin are given for all experiments in Figure 4. Test duration is grouped by soil moisture series, with 8° slope experiments 1 through 3 and 15° slope experiments 4 through 6 corresponding to the same progressive flow increase (low → mid → high). Increases in applied flow caused a general decrease in experiment duration. High slope experiments were somewhat shorter in duration than low slope experiments at the same flow rate. Pre-test soil moisture and post-test water surface slope are not related to the flow condition, but results are presented in this format for uniformity. The C and FT soil moistures were kept very close by preparing and homogenizing a single volume of soil that was divided and placed in each bin. The low, mid, and high soil moisture series are clearly distinguished in Figure 4, but by

design there is very little variation within these series. For the water surface slope results flow conditions 1–3, 4–6, and 7–9 represent increasing flow (low → mid → high) in each soil moisture series. The water surface slopes in the C bins did not change greatly from the initial slopes of 0.176 (8°) and 0.290 (15°) in any test. However, significant slope reductions occurred during several experiments in FT bins, especially in the low moisture series. Post-test soil moisture increased from pre-test levels in the low- and mid-moisture series of experiments, but not in the high-moisture series (Table 1). Post-test soil moisture in the FT bin was generally higher than in the C bin, and increased most significantly from pre-test conditions for the low soil moisture series. These observed soil moisture changes are consistent with the infiltration measurements of the soil characterization.

The calculated time-weighted flow from each bin is related to the “flow condition” designation of Figure 4 in Figure 5 by soil moisture series. This figure provides the precise flows associated with each flow condition. The C and FT flows were essentially equal, with the exception of three mid-moisture experiments where the C bin experienced slightly higher flows. These flow differences are conservative as they favor increased erosion in the C bin relative to the FT. Groundwater depths were all zero in the unsaturated low- and mid-moisture series. Mean groundwater depth measured in FT and C wells before and after each experiment of the saturated high soil moisture series are given in Table 5. These groundwater depths are comparable, with before and FT-bin depths slightly greater than after and C-bin depths, respectively. The pre- and post-experiment data indicate only minor net exchange of water between the surface flow and groundwater in this series. Comparisons between FT and C groundwater depths indicate a negligible difference in surface–subsurface flow exchange between the bins. Minimal surface–subsurface water exchange is consistent with negligible infiltration at high soil moisture in the characterization study.

Integrated Measures of Erosion

The results presented in this section were derived from sediment discharge data for each soil bin and include several concentration measures, load, and total mass. The strength of these global measures is that they integrate the processes occurring in each bin, and are not specific to a particular location. Figures 6, 7, 8, and 9 present mean, time weighted, median, and maximum FT and C outflow sediment concentrations, respectively, with previously defined flow condition, for each slope and soil moisture series. Corresponding dimensionless FT/C ratios of these concentration parameters are also given in each figure. Though parameter values are slightly different, the overall patterns are very similar. Flume experiments of Lei et al. (1998) indicated that sediment concentrations increased with bed slope, but did not generally increase with flow rate. In our experiments there is a strong and consistent dependence in both FT and C concentrations on the bed slope. When other experimental conditions are the same, greater slope produces greater sediment concentrations from both bins. Like Lei et al. (1998) the eroded FT and C concentrations have no clear relationship to flow. The FT/C ratios of these concentrations are all significantly greater than 1, indicating a primary effect of the FT cycle on rill sediment erosion.

Several high soil moisture experiments had C bin concentrations that were low relative to other tests, and corresponding FT/C ratios were large, indicating that FT effects on soil erosion processes are generally maximized at high soil moisture. Low and high soil moisture mean, time weighted, and median

FT concentrations were similar, while corresponding mid-moisture FT concentrations were consistently higher. In contrast, maximum FT concentrations followed soil moisture from high to mid to low. Low and mid soil moisture C concentrations were comparable, while high moisture C concentrations were generally lower. The high moisture series had saturated soil conditions through most of the soil depth, and the highest bulk density. Trends in concentration of eroded soils with soil moisture are not clearly indicated by these results, though erosion resistance increased in the high moisture C series. Our initial interpretation is that the decrease in C erodibility at high soil moisture resulted from greater soil consolidation and/or enhanced cohesiveness.

Time-weighted average sediment loads (g/min) from the FT and C bins during each test and the corresponding FT/C sediment load ratio are presented in Figure 10 with flow condition by slope and soil moisture series. The FT/C ratio reflects significantly higher sediment loads in the FT bins than in the C bins, and a generally increasing effect of FT with soil moisture. Sediment load ratios were in the range from 2 to 4 for the low and mid soil moisture series, and up to 12.7 in the high moisture series. The effects of both flow and slope on FT and C sediment loads are large and apparent in this figure. The high soil moisture FT and C series exhibited generally reduced sediment loads relative to lower soil moisture tests. FT sediment loads of Figure 10 are inversely related to the test durations given in Figure 4. FT/C ratios of mean, median, time-weighted average, and maximum concentrations, and sediment load with flow condition are compared in Figure 11 by slope and soil moisture series. The single valued median and maximum concentration ratios are frequently outliers, while the other measures are comparable. There is a systematic increase in the ratios with soil moisture, clearly indicating an increased importance of FT. The large difference in slope does not produce a trend in FT/C, and trends with applied flow are not consistent between the soil moisture series. Total FT and C sediment sample mass transported during an experiment was obtained by multiplying the average sediment load by test duration. These results and the corresponding FT/C transport ratios are given in Figure 12 with flow condition, by slope and soil moisture series. The C results show generally decreasing total transport with increasing moisture content of the soil, while the FT results do not show a clear trend in total transport with soil moisture. Erosion of the FT bin was used to determine test duration, providing a tendency to equalize the total FT transport of the different soil moisture series. Like sediment load, the total transport generally increased with both flow and slope, while FT/C ratios were not sensitive to these parameters.

The sediment load data of the individual experiments were grouped by soil moisture, slope, and flow to better define trends and relationships, and these results are presented in Table 6. Average sediment load for the complete set of experiments was 37.7 g/min FT and 12.5 g/min C, with a ratio of 3.03. When grouped by soil moisture series, the averaged C load diminished sharply for the high moisture (saturated) soil. The averaged FT sediment load increased from low to mid moisture, and also decreased significantly at high moisture. FT/C ratios 2.41, 3.04, and 4.96 clearly indicate an increasing effect of FT with soil moisture content. A second grouping of the experiments by slope indicates that average FT and C sediment loads were directly proportional to slope. However, the equal FT/C ratios indicate that the effect of FT on sediment load was unrelated to slope. With the experiments grouped according to flow, we observed average FT and C sediment loads that are proportional to flow. Again, the nearly equal FT/C ratios show that the effect of FT on sediment yield was unrelated to flow. The

proportionality of sediment load to flow and slope indicated by these results is consistent with current understanding of rill erosion processes. Large and increasing dimensionless FT/C sediment load ratios with soil moisture highlight the primary role of FT in rill erosion processes that increases with soil moisture.

Local Measures of Erosion

We measured and characterized cross sections of the rills at $0.3L$ (24 cm) and $0.7L$ (55 cm) above the outlet both before and after the flow event. The two norms used to measure cross-sectional change were L_2 , the root-mean-square of the change in bed elevation resulting from the flow, and L_{inf} , the maximum bed elevation change at a point in each cross section. These measures are particular to these specific locations, and might be influenced by local effects that are not representative of the complete reach. To more fully characterize the extent of erosion in each bin, other local measures were obtained to supplement the detailed cross-section measurements. Maximum channel width and maximum channel depth at every $0.1L$ were measured at the conclusion of each experiment and averages are presented here.

L_2 measures for both bins at $0.3L$ and the corresponding FT/C ratio are given in Figure 13 with flow condition by slope and soil moisture series. Corresponding L_{inf} results for this same cross section are given in Figure 14. These same measures at $0.7L$ are given in Figures 15 and 16, respectively. Our initial observation is that both measures are providing very similar information concerning cross-sectional change. The norms indicate very small changes in the controls for both the mid and high soil moisture series, with all norms less than 2.2 and 1 cm, respectively, for these series. The norms for the low soil moisture series in the C bins are also generally small, with $L_2 < 2.5$ cm and $L_{inf} < 3.6$ cm. The upper bound on these C norms decreased as soil moisture increased, indicating generally greater erosion resistance at higher moisture content. The norms of both FT cross sections generally increase with applied flow for the low and mid soil moisture series, and indicate generally enhanced erosion with slope. At high soil moisture the slope dependence of cross-sectional change is again clear, but dependence on flow rate is not apparent. The L_2 and L_{inf} FT/C ratios generally increase with soil moisture, but display no clear dependence on flow or slope. Anomalously high ratios at $0.7L$ for the low moisture, high flow, and low and high slope experiments indicate excessive erosion in that part of the FT bin relative to the same location of the C bin. The ratios of the high soil moisture series are generally high, a result of very minor erosion in the C bins. Greater relative erosion of the C bins in the high flow, high moisture experiments produced the smallest ratios of the group.

Tables 7 and 8 give overall and group-averaged norms and their FT/C ratios for $0.3L$ and $0.7L$, respectively. L_2 and L_{inf} FT/C ratios for the overall experiment are equal (2.81) at $0.3L$, and nearly equal (4.94, 4.56) at $0.7L$, with values much greater than 1 indicating a primary effect of the FT cycle on rill erosion. At $0.3L$ the series-averaged ratios of the L_2 and L_{inf} measures are approximately equal for each moisture series, and increase dramatically with soil moisture. This increase is due largely to significant decreases in the C measures with increasing soil moisture. Rough equality of L_2 and L_{inf} FT/C ratios also occurred at $0.7L$, but the low soil moisture ratios were much larger and comparable to those at high moisture. The high ratios at high moisture are again due to greatly decreased measures in the C bins. Both norms show minor increases for increasing slope groupings at both locations, and corresponding

norm ratios also show relatively small, but consistent, increases with slope. Both measures increase with flow at both locations of the FT bin and in the C bin at $0.3L$. There are no trends in either FT/C ratio for $0.3L$, but these ratios show a general increase with flow at $0.7L$. These results are generally consistent with the measures obtained for group-averaged sediment load, but the trends are not as simple and clean. The importance of FT induced erosion and its dependence on soil moisture is a consistent theme.

Nine-point averages of maximum channel width and maximum channel depth were obtained and are presented with flow condition in Figures 17 and 18, respectively, by slope and soil moisture series. Average maximum channel width (Fig. 17) generally increases with flow and slope in both bins. The average maximum widths in each bin were generally highest at mid soil moisture, and comparable at both higher and lower soil moisture. Corresponding FT/C ratios generally increase with soil moisture and do not display trends with flow or slope. Average maximum channel depth (Fig. 18) generally decreases with increasing soil moisture, increases with slope, and has some dependence on flow. Corresponding FT/C ratios again generally increase with soil moisture, but do not depend on flow or slope. Group-averaged maximum rill widths and depths in Table 9 were obtained for soil moisture, slope, and flow, as well as overall. Grouped maximum rill widths increased with both slope and flow. However, the FT/C ratios indicate that only soil moisture caused a width change as a result of FT, and then only at high soil moisture. Trends in grouped maximum rill depth are very similar to those of sediment load. Again, the important effect of soil moisture change on FT effects is clearly indicated by the FT/C depth ratio, while increasing slope and flow cause depth increases that are unrelated to FT. Overall, depth differences between FT and C bins are greater than those of width, but trends in these parameters and their ratios are similar. Trends in these parameters are also similar to those of the L_2 and L_{inf} cross-sectional measures.

Replication of Experiments

Part way through our experimental program it became clear that the outcome of a particular experiment was greatly affected by the parameters that describe the condition of the soil bins. To obtain results that could be quantitatively compared and interpreted required minimum differences between all bins of each soil moisture series, including weight, bulk density, and soil moisture. As evidenced by nonzero standard deviations in Table 1, these parameters could not be replicated exactly, especially the soil moisture. In this section we compare three experiments that were approximately replicated to better understand and quantify the relationship between variability in parameters and corresponding variability in results. Parameter differences considered here are generally larger than the corresponding standard deviations of our experimental series. Low moisture experiment 6 and high moisture experiment 4 listed in Table 10 were included in the analysis above. The replicate of low moisture experiment 6 had significantly lower soil weight, lower soil moisture, and higher applied flow. High moisture experiment 4 and its replicate were more similar, with a large difference only in soil moisture. Corroborating the difference in FT soil moisture was an average groundwater level difference of 12 cm to 3 cm between these replicates. Groundwater levels in both C bins were 12 cm. This same experiment was repeated twice more at lower soil weight and volume, at about the same bulk density as the original, and was called high moisture experiment 4–light. These two experiments have the closest parameters of the group, differing only in soil moisture by slightly more than the standard deviation of the high moisture series

(Table 1). There was a small difference in FT groundwater levels, with 10 cm and 7 cm in the higher and lower moisture replicates, respectively, while C levels were both 10 cm. This final comparison should provide an upper bound on the uncertainties in results for individual experiments of this study.

Equations used to quantify the differences between results for the pairs of replicated experiments were the same for FT and C comparisons. The dimensional difference in each quantity for corresponding FT bins can be expressed as

$$\Delta FT = \left| FT - FT_{\text{rep}} \right| \quad (1)$$

where subscript “rep” indicates replicate, and the dimensionless percentage difference in FT quantities is

$$\Delta FT / FT = \frac{\left| FT - FT_{\text{rep}} \right|}{FT} \quad (2)$$

Results of comparisons using (1) and (2) are given in Table 11 for mean, time weighted, median, and maximum sediment concentration, sediment load, total sediment transport, L_2 and L_{inf} norms at $0.3L$ and $0.7L$, and average maximum width and depth. ΔFT and ΔC are expressed in Table 11 in the same units as the original quantities, g/L for concentrations, g/min for load, kg for total transport, and cm for norms, width, and depth.

Low moisture experiment 6 replicates showed good agreement in FT concentrations, total transport, and norms at $0.3L$. However, differences in the C replicates are generally large, especially in the norms, with lower soil weight and higher flow yielding significantly more erosion. We offer the interpretation that reduced soil moisture negates reduced soil weight and increased applied flow in the FT, but not in C where changes in soil moisture are less important. High soil moisture experiment 4 and its replicate indicate greatly increased FT concentrations and sediment load at higher moisture. Cross-sectional changes were not as large in the FT, and ΔC quantities were generally small. Changes in soil moisture of several percent by volume can greatly affect the erosion rate following FT. High soil moisture experiment 4–light comparisons indicate generally small dimensional changes between the replicates, with concentrations differing by < 3 g/L and cross-section measures by < 0.5 cm. Percentage changes can be large for parameters where the quantity being measured is small. The larger soil moisture replicate produced small, but consistent increases in all FT and C quantities. These replicate comparisons confirm our general observation that experimental results converge as parameter variability decreases, and verify that tight parameter control within experimental series will permit quantitative comparisons of results. However, even with tightly controlled experiments, small differences in results are expected between replicates that for small quantities may result in large percentage changes.

Very Low Moisture Experiment

Our results have shown that a FT cycle has primary effects on subsequent flow-induced erosion for soil moistures ranging from 17–39% by volume, and that these effects increase with soil moisture

through this range. Conversely, it may be anticipated that FT effects on Hanover silt or any other soil would diminish and eventually disappear as soil moistures approach zero. To test this hypothesis we repeated an experiment from the low moisture series at greatly reduced soil moisture. The soil in this experiment was visibly much drier than that of the low moisture series. Both the conditions and results of this low moisture 2–dry experiment are presented in Table 12. The conditions include low slope, mid flow, and soil moistures in the 4–5% by volume range. The FT/C ratio of each concentration measure is slightly greater than 1, indicating marginal increases in soil erosion as a result of FT. The absolute and percentage increases in FT relative to C concentrations are also relatively small for this “dry” experiment. For comparison, the FT/C ratios of each concentration measure for the corresponding low moisture experiment all exceed 2. The dry experiment sediment load and total transport also increased by just a few percent in the FT relative to the C, while increases in the corresponding low moisture experiment were more than double. Dry experiment cross-sectional measures also provide very similar comparisons that indicate only slightly greater erosion of the FT. Differences between the dry and low moisture experiments show convergence of the various FT and C erosion measures as soil moisture approaches zero, and greatly reduced effects of FT on rill erosion. These results confirm the fundamental importance of soil moisture to FT-induced changes in soils that affect subsequent flow-induced erosion.

Summary and Conclusions

In this paper we quantitatively tested the hypothesis that soil FT processes can significantly increase the potential for upland hillslope erosion during runoff events that follow thaw. Our conceptual understanding is that ice formed in soil voids during freezing reduces particle cohesion and soil strength, and makes the soil more erodible. Frost-susceptible silt was used to obtain an upper bound on increases in bare soil erodibility and rill development due to a single FT cycle over ranges of soil moisture, applied flow, and slope. For each experiment identical soil bins, an unfrozen control (C), the other frozen and thawed, were tested in parallel to quantify FT effects. Standard soil characterization tests were unable to detect significant differences between FT and C soils, especially at high (saturated) soil moisture where increases in erosion were the greatest. Important changes caused by FT to enhance soil erodibility must occur at smaller scales than those of the tests, probably approaching that of an ice lens, soil grain, or pore. Measurements at these scales have a greater potential to be definitive. Without small-scale measurements we cannot advance understanding of soil FT mechanics, and instead focus on quantifying the effects.

Three replicated experiments showed a convergence of results as differences in bin weight, bulk density, and soil moisture decreased. To support quantitative comparisons of results, tightly controlled bin preparation minimized these differences over all soil bins of each prescribed soil moisture series of experiments. Sediment load obtained from runoff samples gave an integrated measure of erosion through time for each bin, while cross-sectional data provided measures of erosion at specific locations. Both types of data were obtained to provide independent evidence, allowing us to assess the concurrence of trends, and yield a stronger basis for conclusions. The maximum eroded rill width and depth averaged for nine locations, root-mean-square and maximum rill cross-sectional depth change for two locations, and average sediment loads and total mass transport during each experiment were all greatly increased by the

FT cycle, reflected by average FT/C ratios for the full series of experiments between 1.2 and 4.9. These results leave little doubt that soil FT is of primary importance to overland flow-induced erosion following thaw. These measures all followed similar trends when grouped and averaged for equal soil moisture, slope, and flow. Average FT and C trends both increased with slope and flow when those data groupings were considered. Approximate proportionality of sediment load to slope and flow is consistent with current understanding of rill erosion. However, grouping by slope and flow yielded a consistent relationship between FT and C parameters, represented by the corresponding FT/C ratio. All these FT/C ratios were nearly equal to the overall ratio for the complete set of experiments, indicating that the effects of FT were independent of both slope and flow. The only experimental variable that affected the relationship between FT and C for each of the measured parameters was soil moisture. Sediment load and rill measurement FT/C ratios increased dramatically with soil moisture content. As an example, averaged sediment load ratios increased from 2.4 to 5.0 over the soil moisture range considered. In addition, an experiment at very low soil moisture, 4.4% by volume, yielded an FT/C ratio of 1.02, indicating minimal FT effects in very dry soils. These results confirm that soil moisture is the primary parameter controlling the enhancement of frost-susceptible soil erosion following FT. Because the soil used in our experiments was frost-susceptible, the effect of FT on erosion was probably near its maximum.

The results of this paper demonstrate that FT is a primary process contributing to upland soil erosion in cold climates, and that FT effects can increase up to several hundred percent with soil moisture. Watersheds or sub-watersheds with high soil moisture and silty soils that freeze have greatly enhanced erodibility during runoff events that follow thaw. These results also suggest that models of flow-induced rill erosion must properly account for the effects of FT in order to successfully predict hillslope erosion and sediment yield for watersheds that experience ground freezing. Algorithms that accurately describe near-surface soil moisture and moisture redistribution during freezing and thawing are required elements of such models. Analysis of these experimental data will continue with goals that include parameterization of FT effects on soil erosion, and quantitative comparison with existing models of FT effects. Further investigation of fundamental FT effects on flow-induced soil erosion for other soils and at larger scales would expand on the results presented here.

Acknowledgements

The authors thank Dennis Lambert for his help in designing and fabricating the CRREL soil-erosion simulator, and Lauren Raymond and Reed Harrison for assistance in conducting the experiments and analyzing the samples. Funds for this research were provided by the Engineer Research and Development Center Regional Sediment Management project “Freeze–Thaw Effects on Soil and Bank Erosion and Stability,” and BT25 project “Soil Erodibility and Runoff Erosivity Due to Soil Freezing and Thawing.”

References

- Anderson DM, Pusch R, and Penner E. 1978, *Geotechnical Engineering for Cold Regions*. McGraw-Hill, New York: 566p.
- Benoit GR, and Voorhees WB. 1990. Effect of freeze–thaw activity on water retention, hydraulic conductivity, density, and surface strength of two soils frozen at high water content. *In Proc. Int. Symp. on Frozen Soil Impacts on Agricultural, Range and Forest Lands* (KR Cooley, ed.), US Army Cold Regions Res. Eng. Lab. Spec. Rept., 90-1: 45–53.
- Bryan RB. 2000. Soil erodibility and processes of water erosion on hillslope. *Geomorphology*, 32: 385–415.
- Chamberlain EJ. 1981. Frost susceptibility of soil, review of index tests. US Army Cold Regions Res. Eng Lab. Monog., 81-2: 110p.
- Edwards LM, and Burney JR. 1987. Soil erosion losses under freeze/thaw and winter ground cover using a laboratory rainfall simulator. *Canadian Agricultural Engineering*, 29(2): 109–115.
- Edwards LM, Burney JR, and Frame PA. 1995. Rill sediment transport on a Prince Edward Island (Canada) fine sandy loam. *Soil Technology*, 8: 127–138.
- Elliot WJ, Olivieri LJ, Laflen JM, and Kohl KD. 1990. Predicting soil erodibility from soil strength measurements. ASAE Summer Meeting Paper No. 90-2009, Columbus, OH.
- Formanek GE, McCool DK, and Papendick RI. 1984. Freeze-thaw and consolidation effects on strength of a wet silt loam. *Transactions of the ASAE*, 27(6): 1749–1752.
- Gatto LW. 2000. Soil freeze-thaw induced changes to a simulated rill: potential impacts on soil erosion. *Geomorphology*, 32: 147–160.
- Janson L. 1963. *Frost Penetration in Sandy Soil*. Elanders Boktryckeri, Goteborg, Sweden: 165p.
- Jumikis AR. 1962. *Soil Mechanics*. Van Nostrand, Princeton, New Jersey: 791p.
- Kok H, and McCool DK. 1990. Freeze–thaw effects on soil strength. *In Proc. Int. Symp. on Frozen Soil Impacts on Agricultural, Range and Forest Lands*. (KR Cooley, ed.), US Army Cold Regions Res. Eng. Lab. Spec. Rept. 90-1: 70–76.
- Lal R, and Elliot W. 1994. Erodibility and erosivity. *In Soil Erosion Research Methods*. (R Lal, ed.), Soil Water Conserv. Soc., St. Lucie Press, Delray Beach, Florida: 181–208.
- Lei T, Nearing MA, Haghghi K, and Bralts VF. 1998. Rill erosion and morphological evolution: a simulation model. *Water Resources Research* 34(11): 3157–3168.

Pall R, Dickinson WT, Green D, and McGirr R. 1982. Impacts of soil characteristics on soil erodibility, Recent Developments in the Explanation and Prediction of Erosion and Sediment Yield. *IAHS Publ. No.* 137: 39–47.

Radke, JK, and Berry, EC. 1997. Freezing and thawing effects on soil water and solute movement in repacked soil columns. In *Int. Symp. On Physics, Chemistry, and Ecology of Seasonally Frozen Soils*. (IK Iskandar, EA Wright, JK Radke, BS Sharratt, PH Groenevelt, and LD Hinzman, eds.), Proc. Fairbanks, Alaska Symp., June 1997, US Army Cold Regions Res. Eng. Lab. Spec. Rept. 97-10: 17–23.

Shoop SA, and Gatto LW. 1992. Geology and geohydrology at CRREL, Hanover, New Hampshire, Relationship to subsurface contamination. U.S. Army Cold Regions Res. Eng. Lab. Special Report 92-24, 89 pp.

Van Klaveren RW. 1987. Hydraulic erosion resistance of thawing soil. PhD dissertation, Washington State University, Pullman, WA.

Van Klaveren RW, and McCool DK. 1998. Erodibility and critical shear of a previously frozen soil. *Transactions of the ASAE*. 41(5): 1315–1321.

Figures

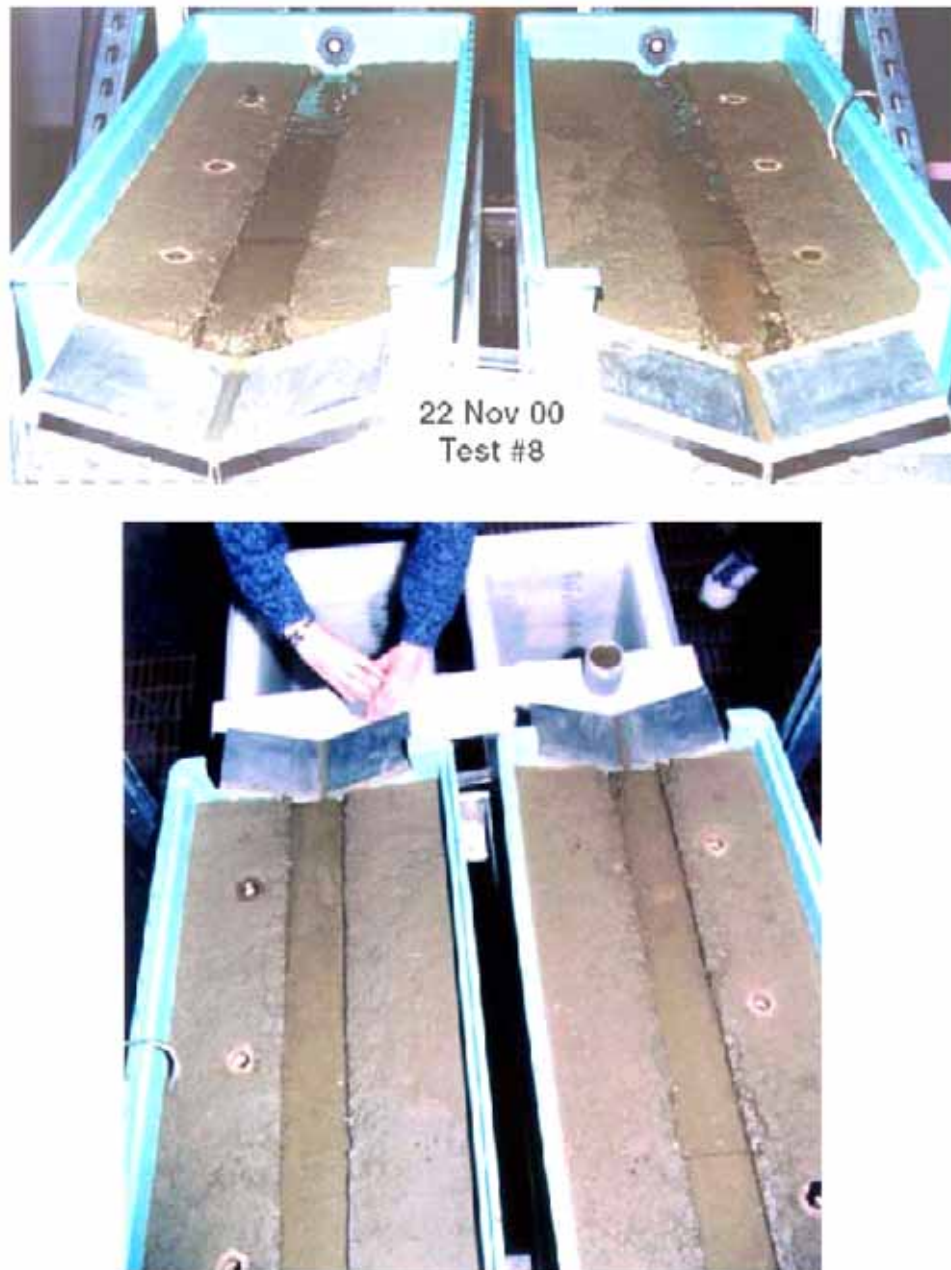


Figure 1. Experimental setup: a) CRREL soil-erosion simulator looking upstream with FT bin on right and C bin on left, and b) discharge receiving reservoirs (white) below the soil bins. Note the flow inlet, imposed rectangular rill, downstream weir, and groundwater wells in each bin, and discharge/sediment sample collection.

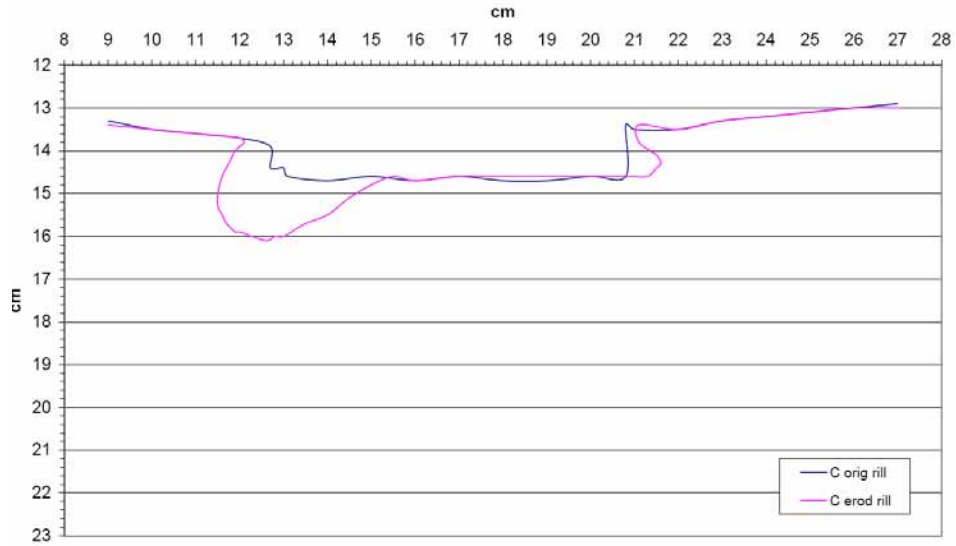


Figure 2. Cross sections of imposed and eroded rills at 55 cm ($0.7L$) above the outlet in the FT and C bins for the mid-moisture, 15° -slope, high-flow experiment.



Figure 3. Typical development sequence of an eroding rill: a) shallow sheet flow across the imposed rill, b) parallel multi-channel flow, c) single enlarged channel flow with sliding pin meter shown, and d) knickpoint formation in the FT (right) bin.

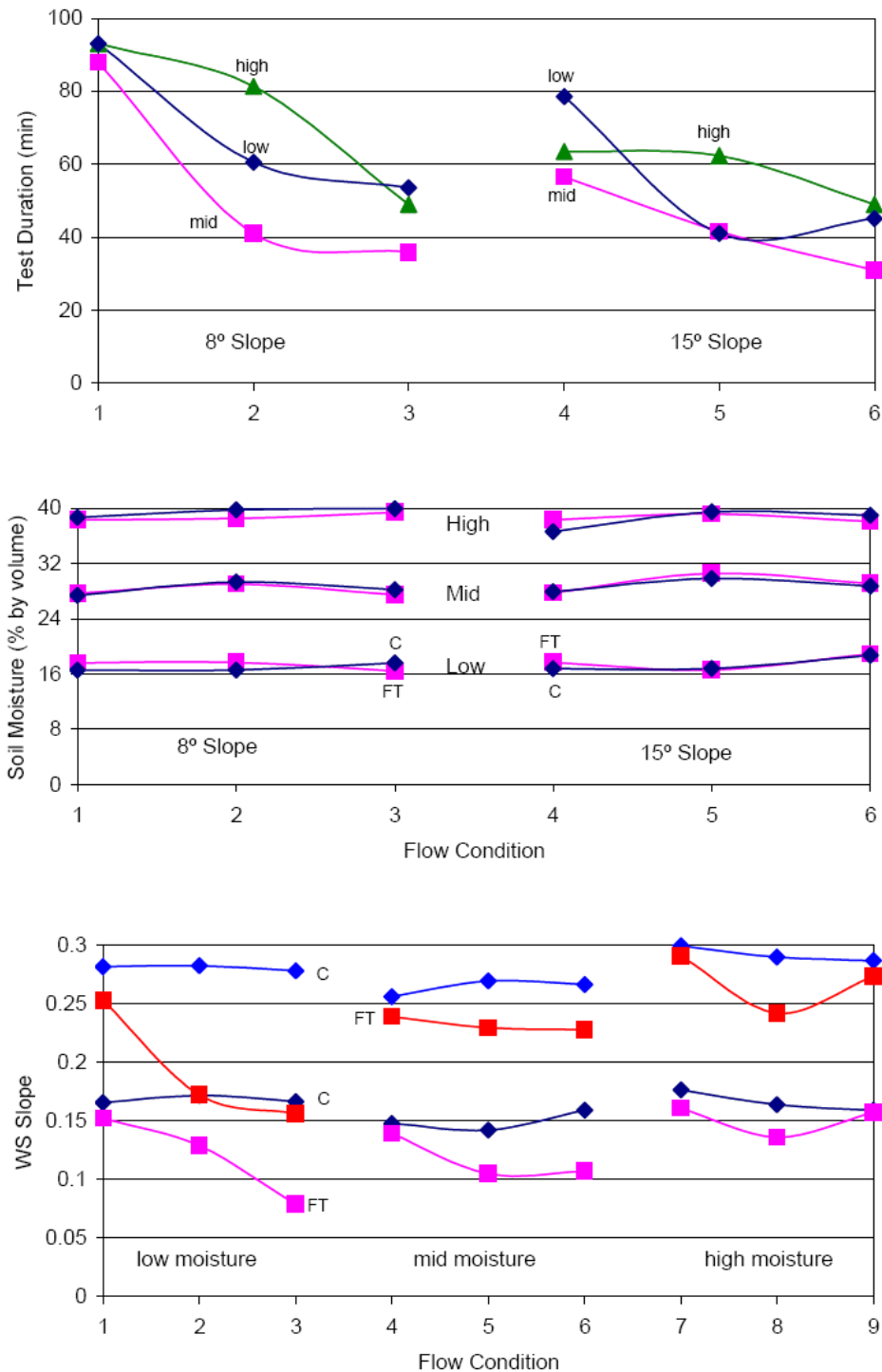


Figure 4. Test duration (min) of each soil moisture series (low, mid, high) plotted against flow condition, where tests 1–3 and 4–6 represent low, mid, and high flow conditions, respectively, for 8° slope and 15° slope conditions. Pre-test C and FT soil moisture contents with flow condition (1–3, 4–6) for each slope condition. Post-test C and FT water surface slopes with flow condition (1–3, 4–6, 7–9) for each soil moisture series.

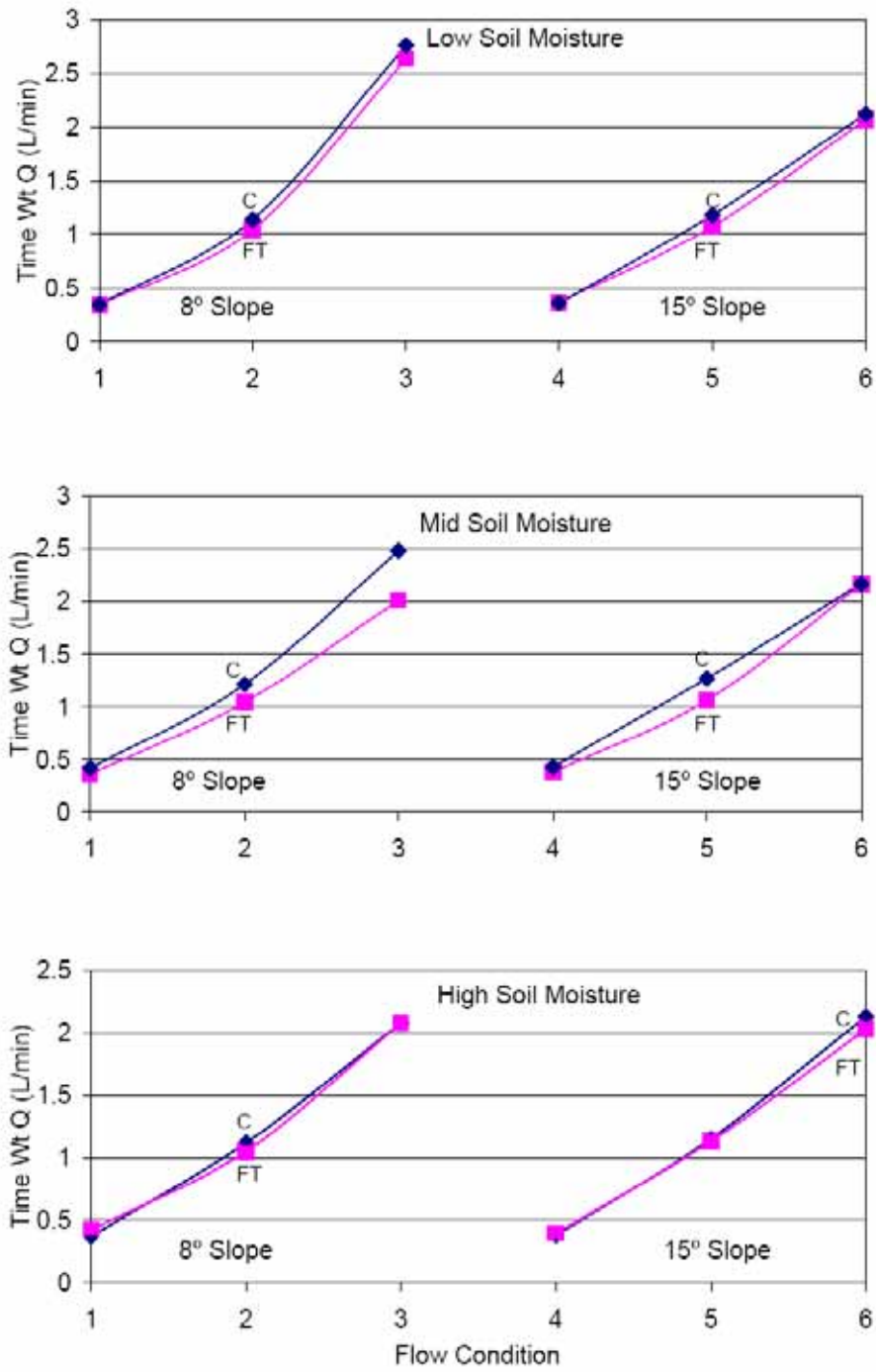


Figure 5. Time weighted discharge (L/min) from each bin related to flow condition by slope and soil moisture series.

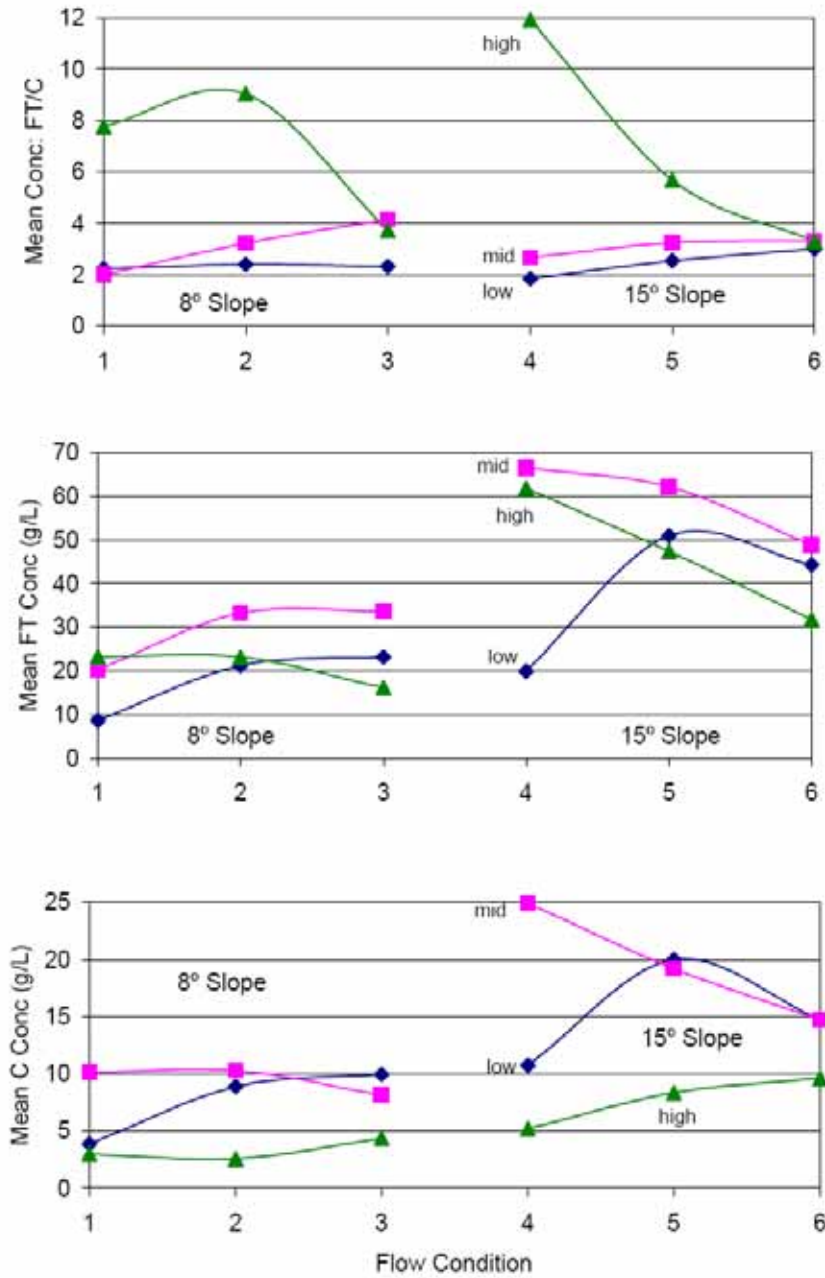


Figure 6. Mean FT and C runoff sample sediment concentrations (g/L) and FT/C ratio with flow condition, by slope and soil moisture series.

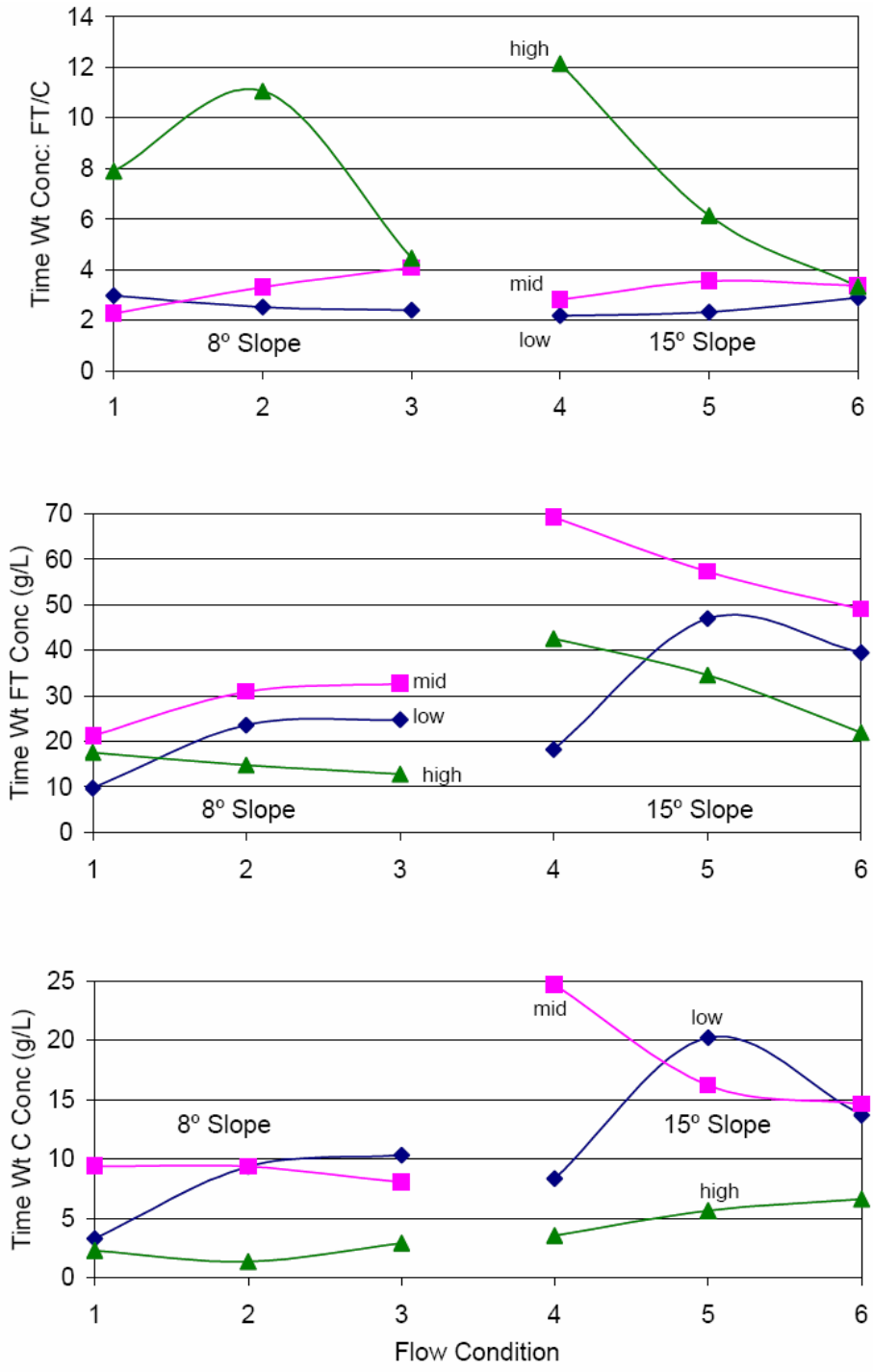


Figure 7. Time-weighted FT and C runoff sample sediment concentrations (g/L) and FT/C ratio with flow condition, by slope and soil moisture series.

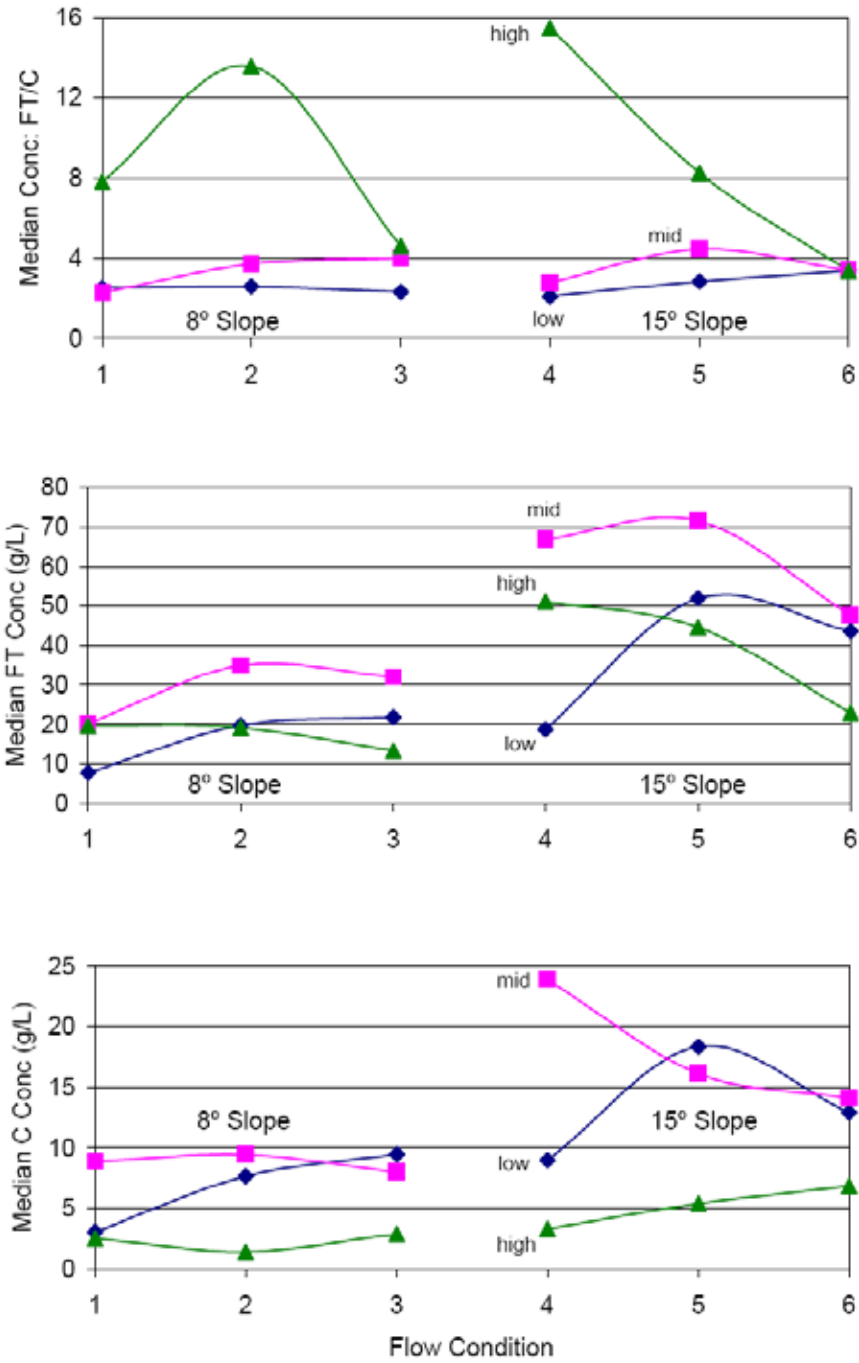


Figure 8. Median FT and C runoff sample sediment concentrations (g/L) and FT/C ratio with flow condition, by slope and soil moisture series.

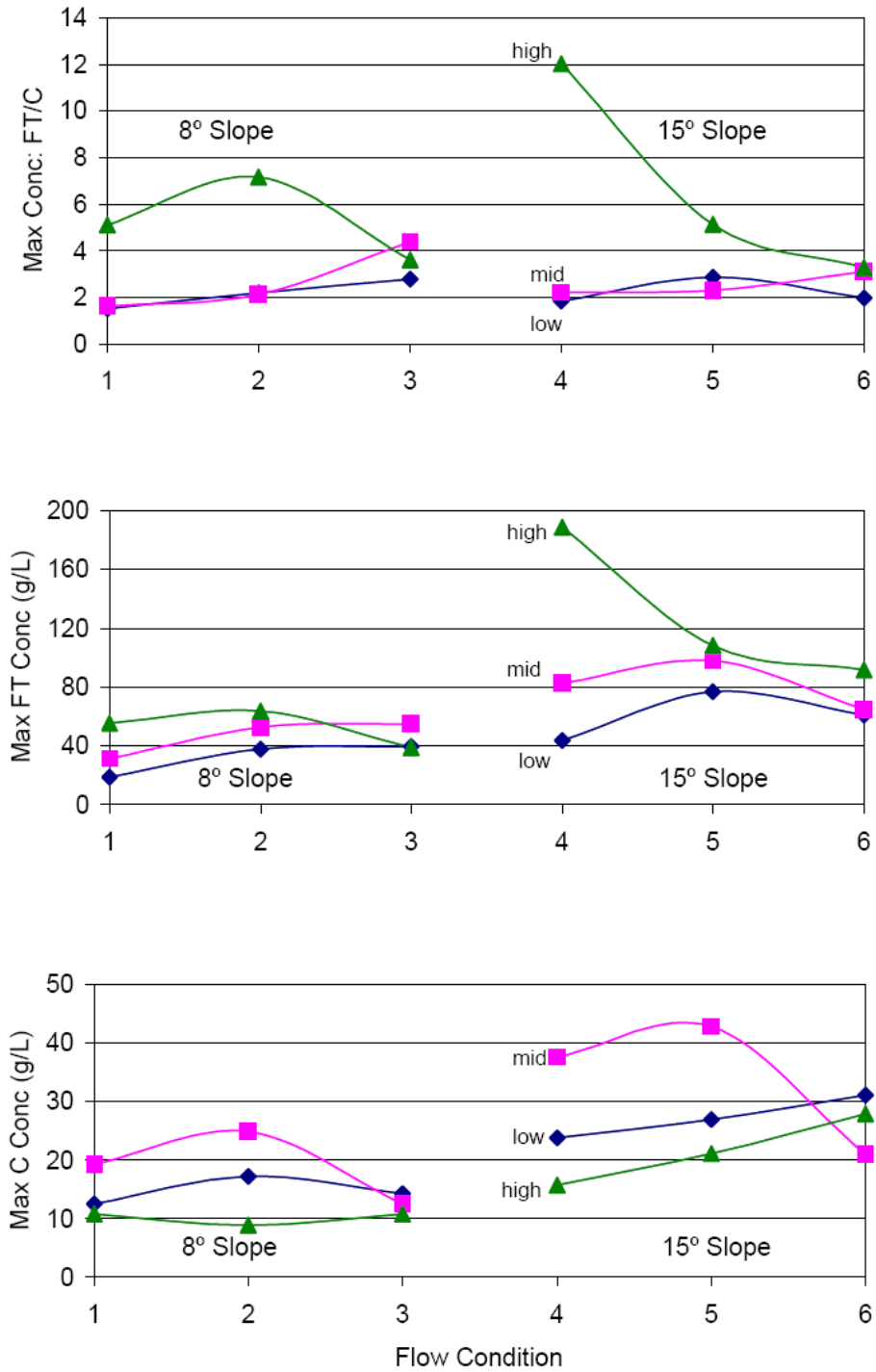


Figure 9. Maximum FT and C runoff sample sediment concentrations (g/L) and FT/C ratio with flow condition, by slope and soil moisture series.

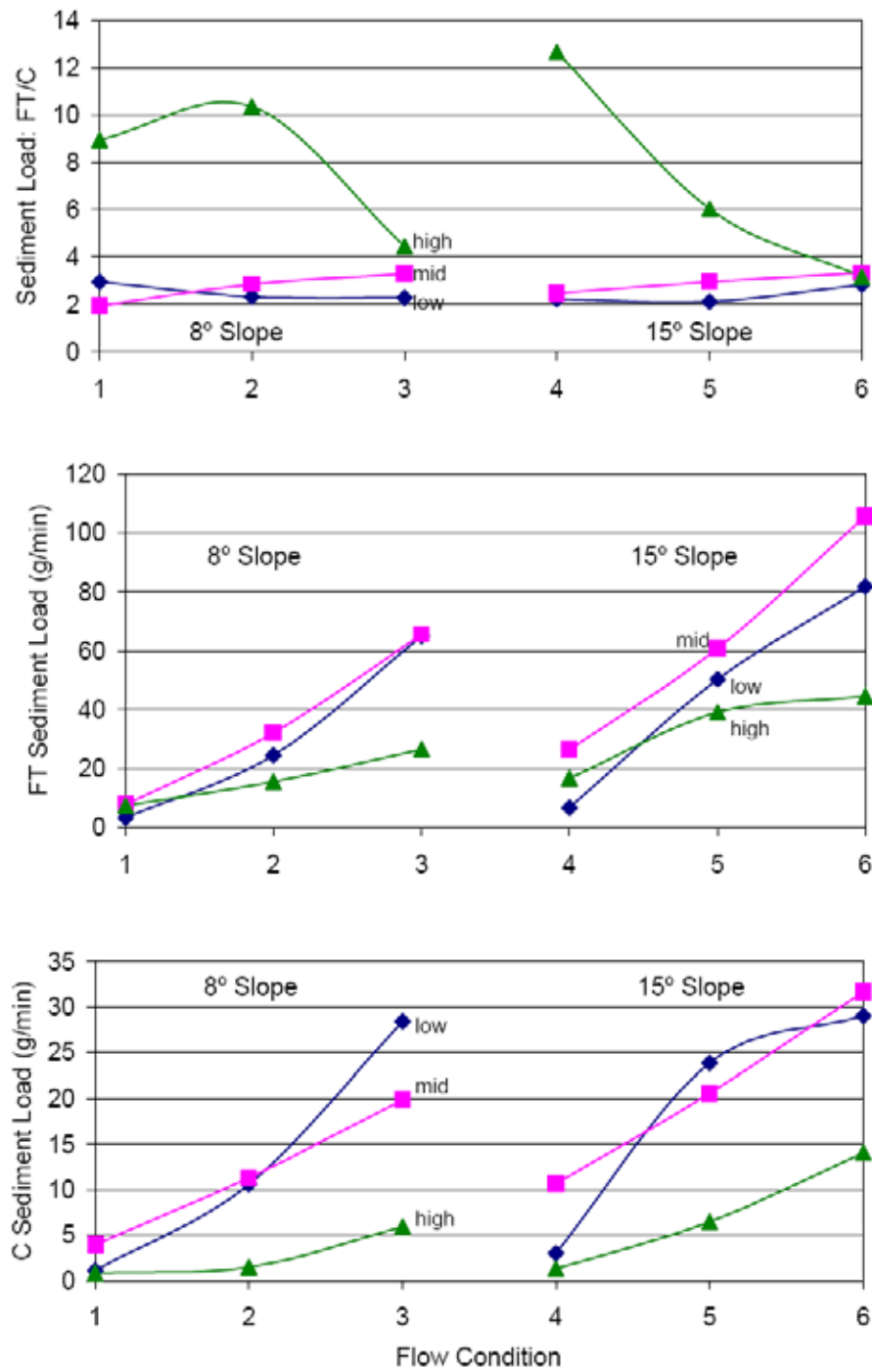


Figure 10. Time-weighted FT and C sediment loads (g/min) and FT/C ratio with flow condition, by slope and soil moisture series.

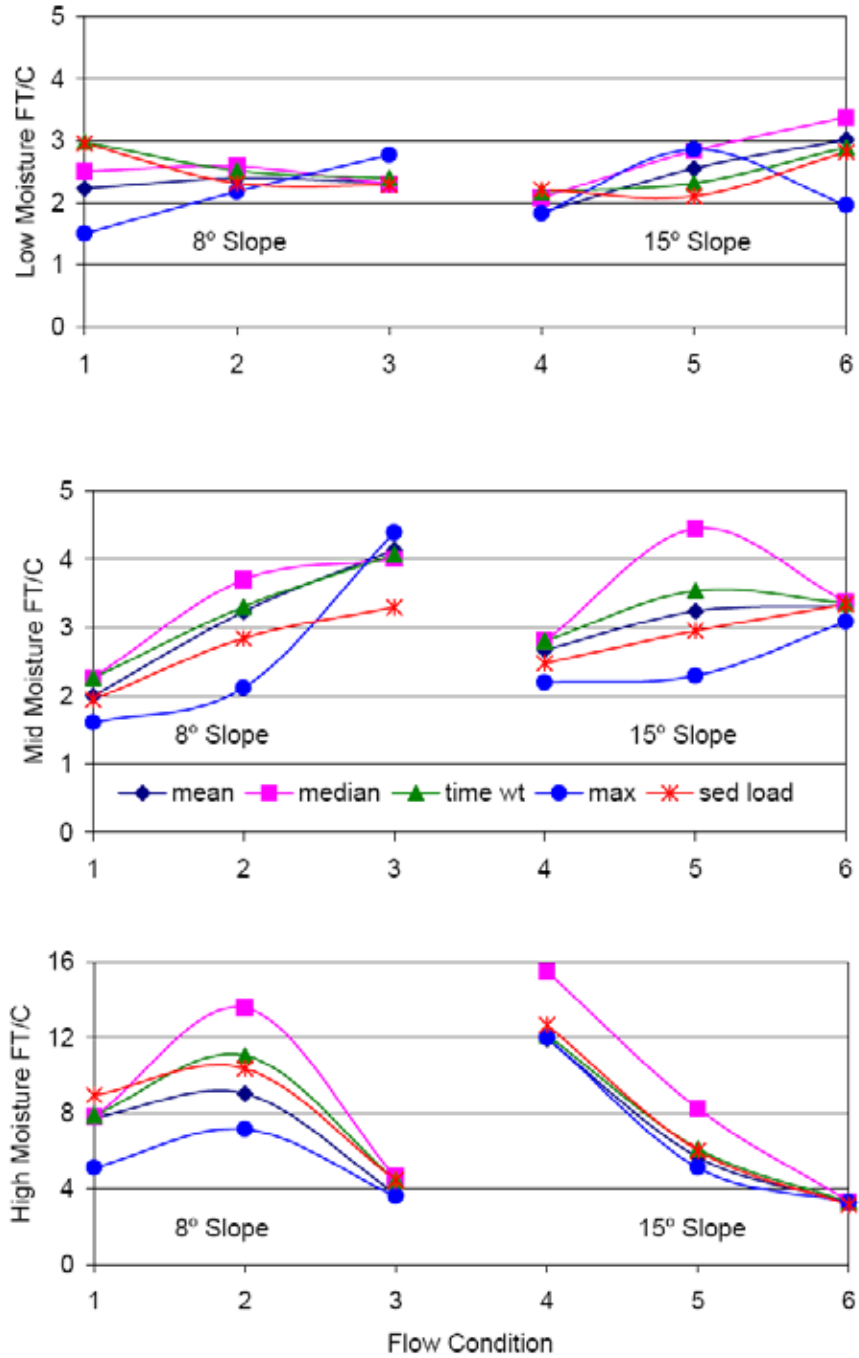


Figure 11. FT/C ratios for mean, time-weighted, median, and maximum concentration, and sediment load with flow condition, by slope and soil moisture series.

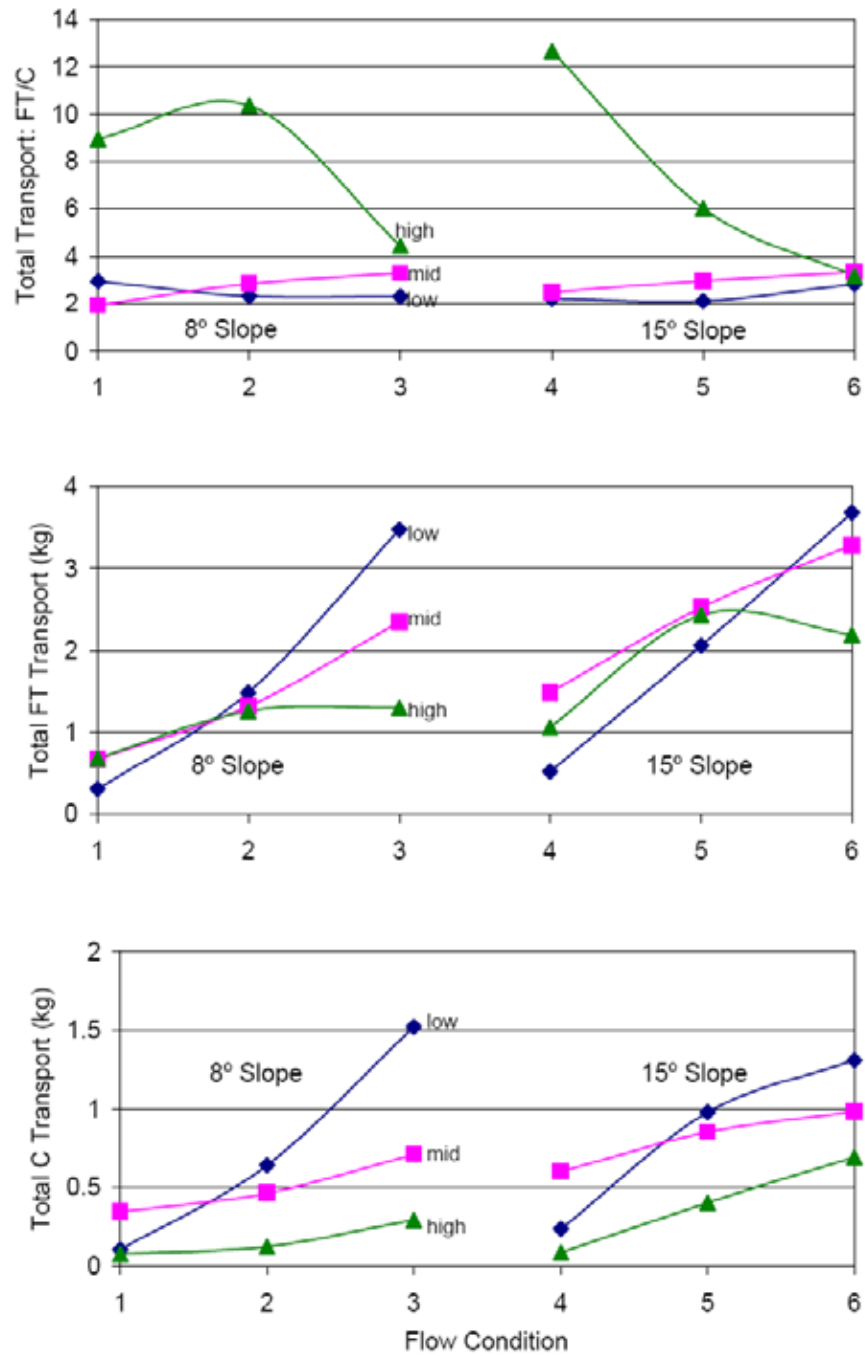


Figure 12. Total FT and C sediment transport (kg) and FT/C ratio with flow condition, by slope and soil moisture series.

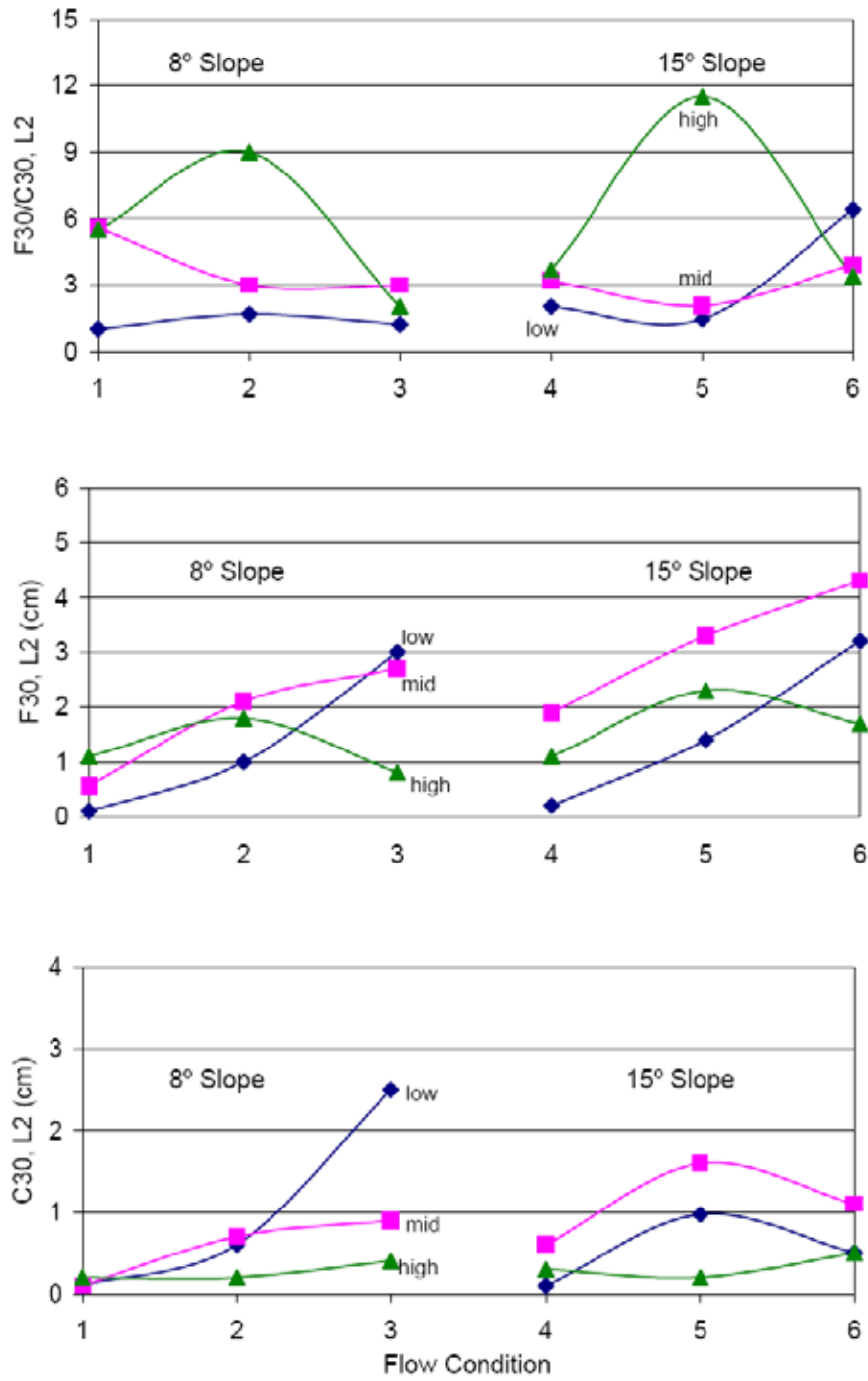


Figure 13. FT and C_{L2} norms of the section at $0.3L$ above the outlet and FT/C ratio with flow condition, by slope and soil moisture series.

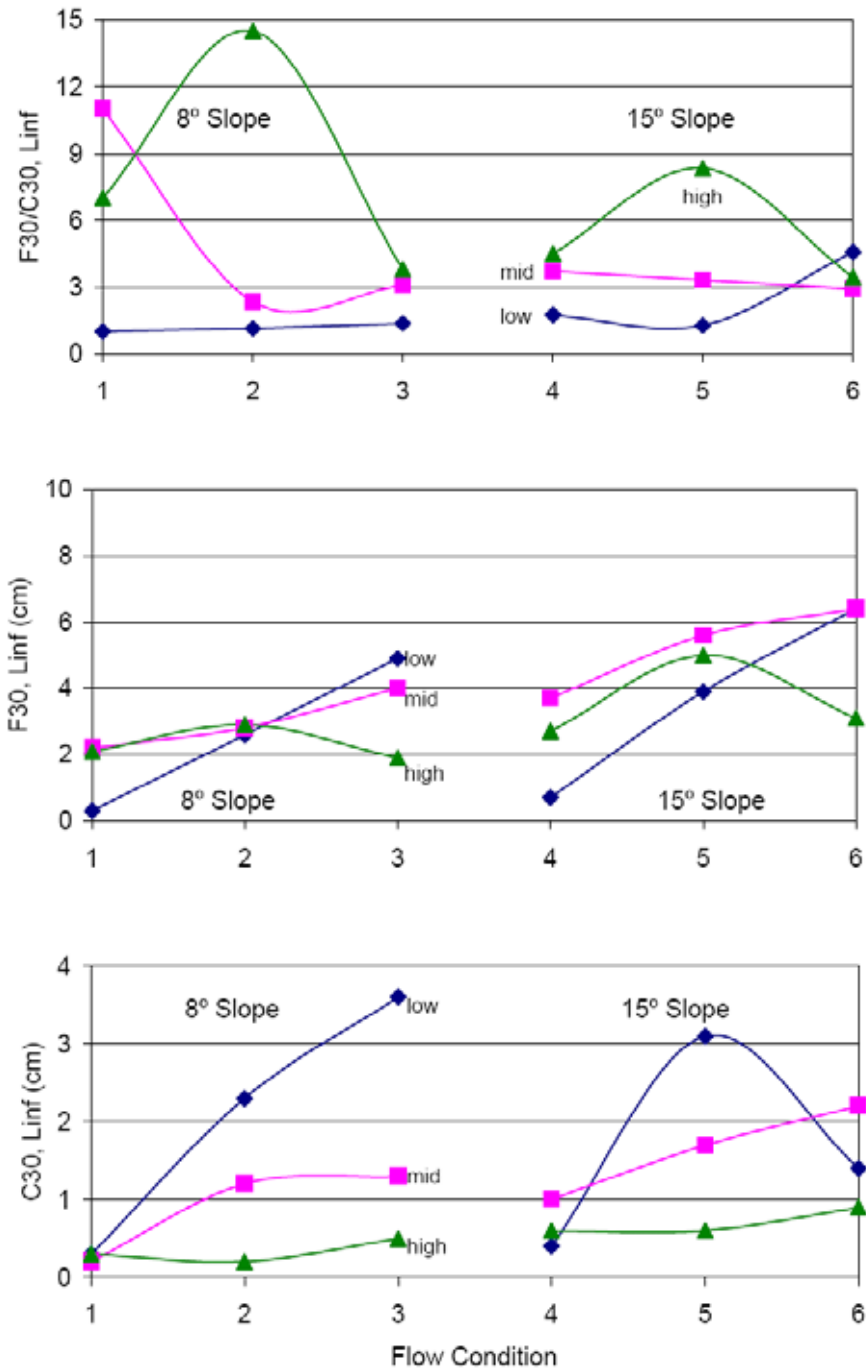


Figure 14. FT and C L_{inf} norms of the section at $0.3L$ above the outlet and FT/C ratio with flow condition, by slope and soil moisture series.

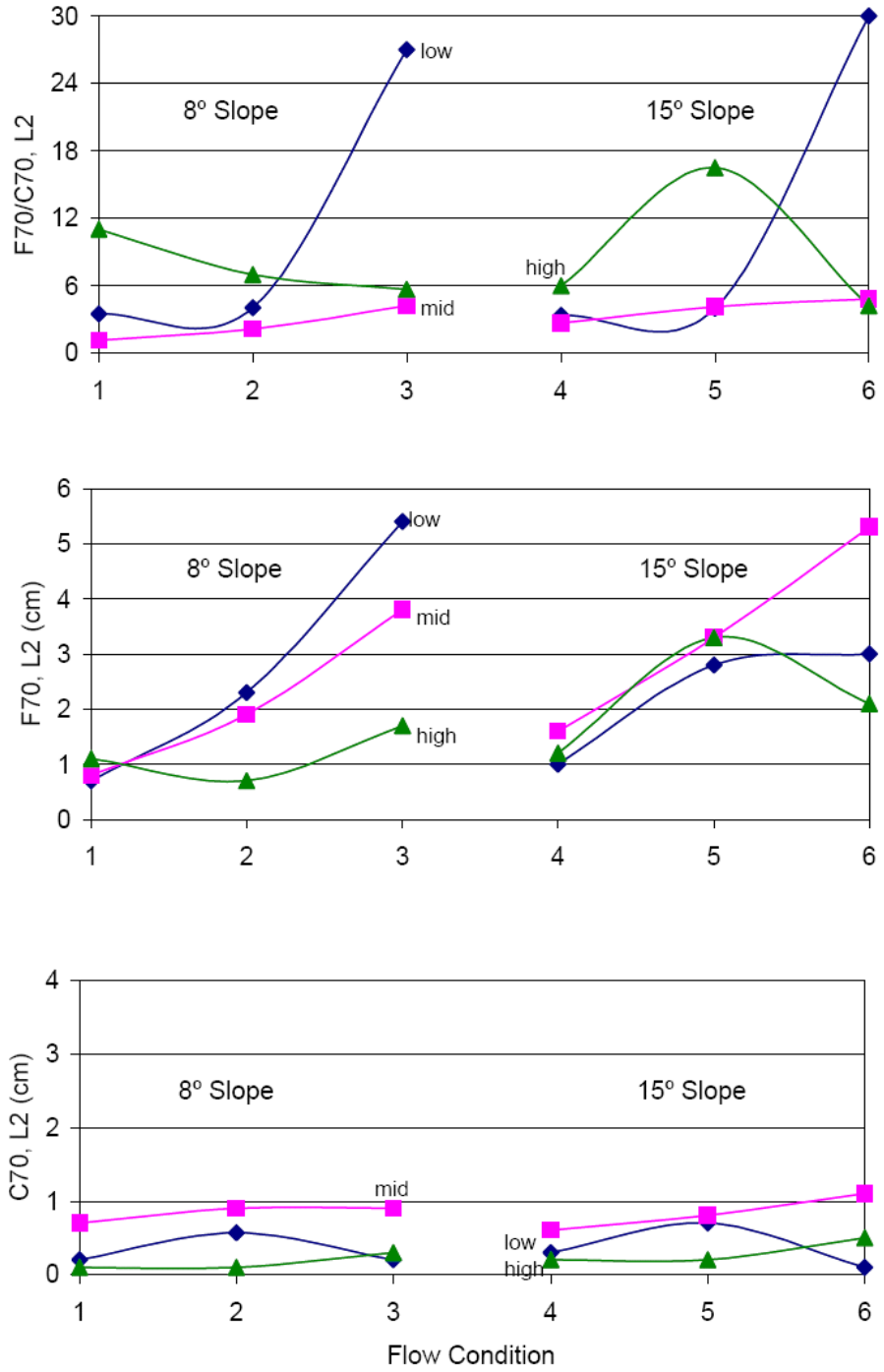


Figure 15. FT and C L_2 norm of the section at $0.7L$ above the outlet and FT/C ratio with flow condition, by slope and soil moisture series.

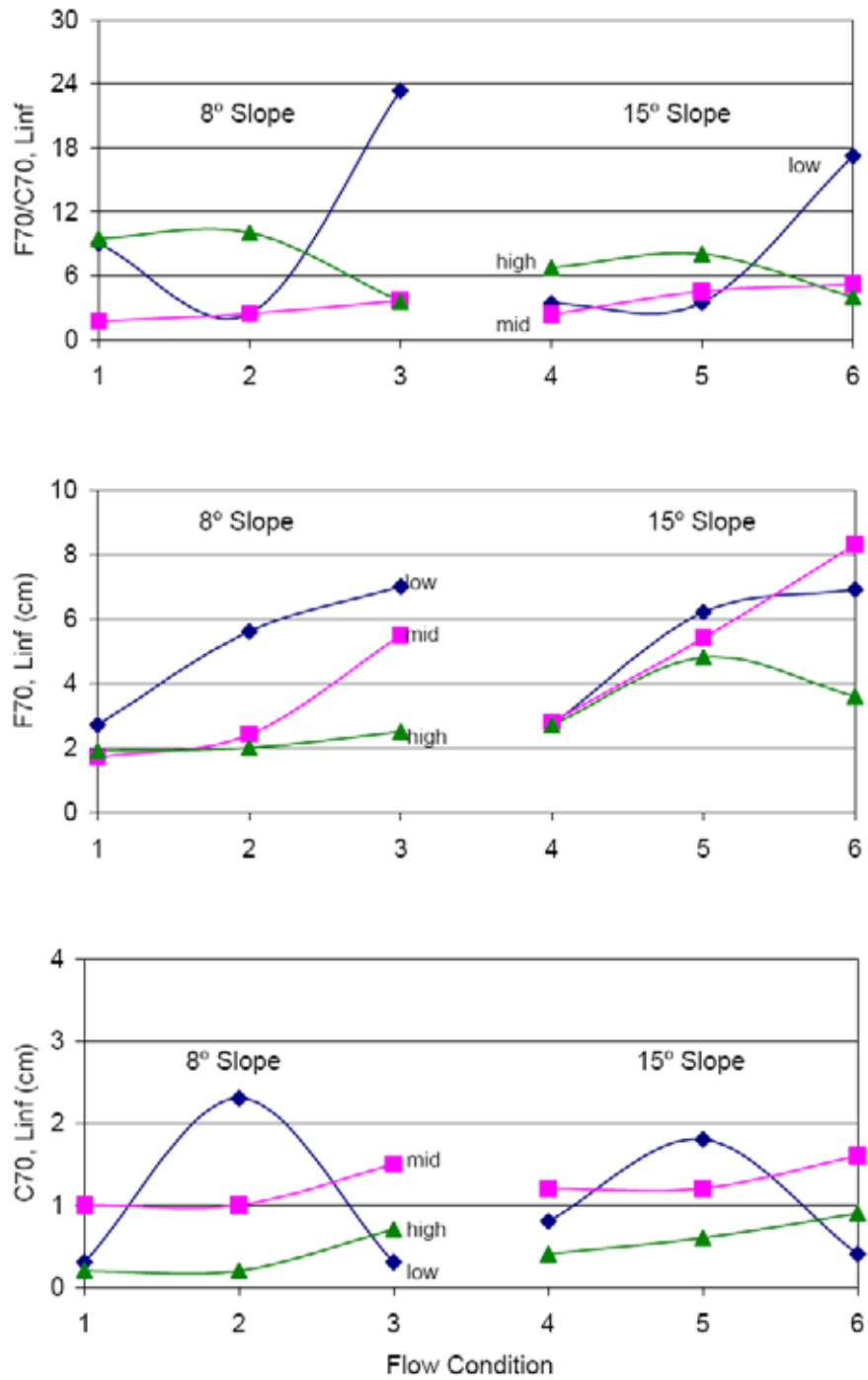


Figure 16. FT and C L_{inf} norm of the section at $0.7L$ above the outlet and FT/C ratio with flow condition, by slope and soil moisture series.

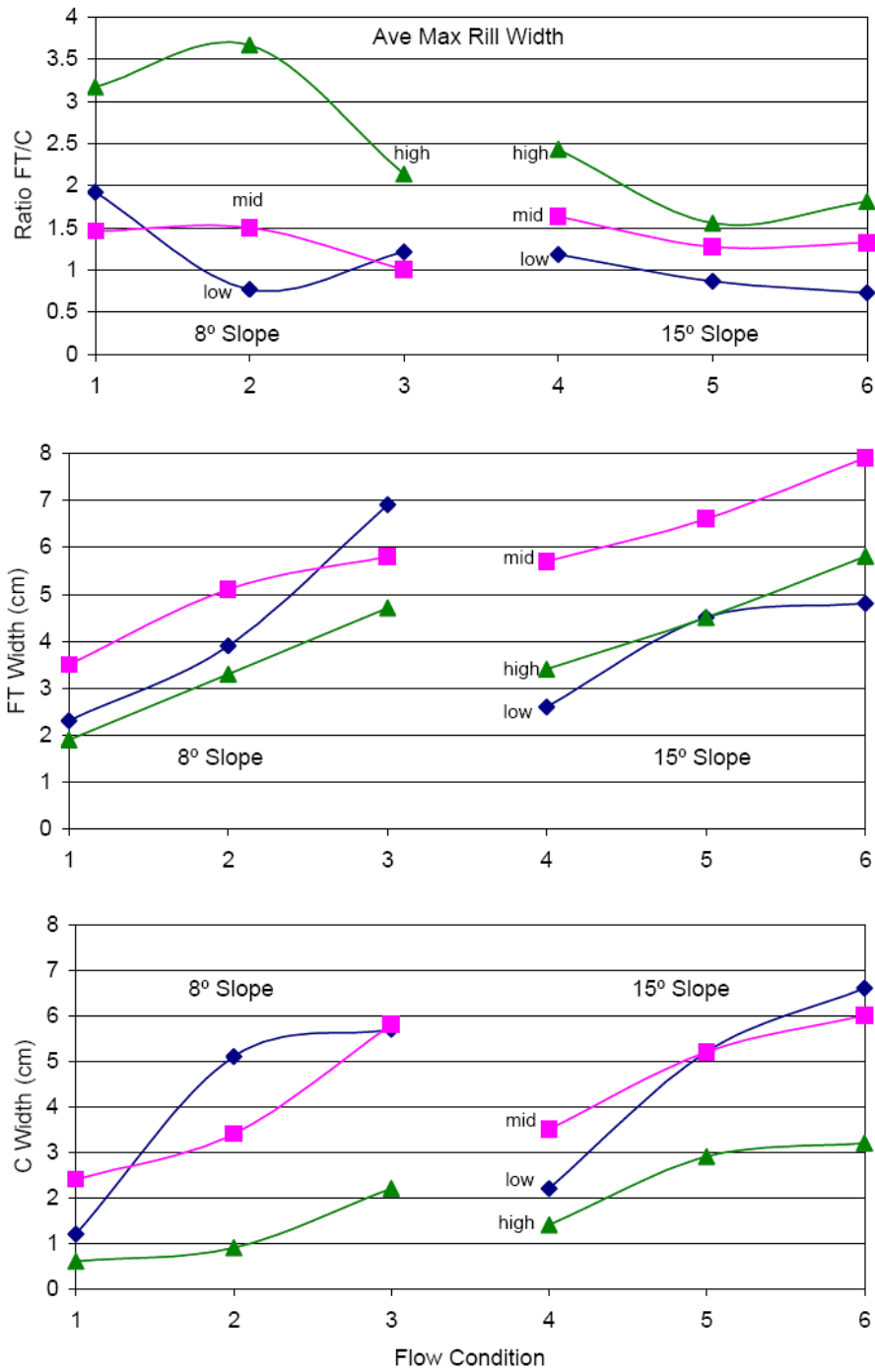


Figure 17. Average maximum FT and C rill width and FT/C ratio with flow condition, by slope and soil moisture series.

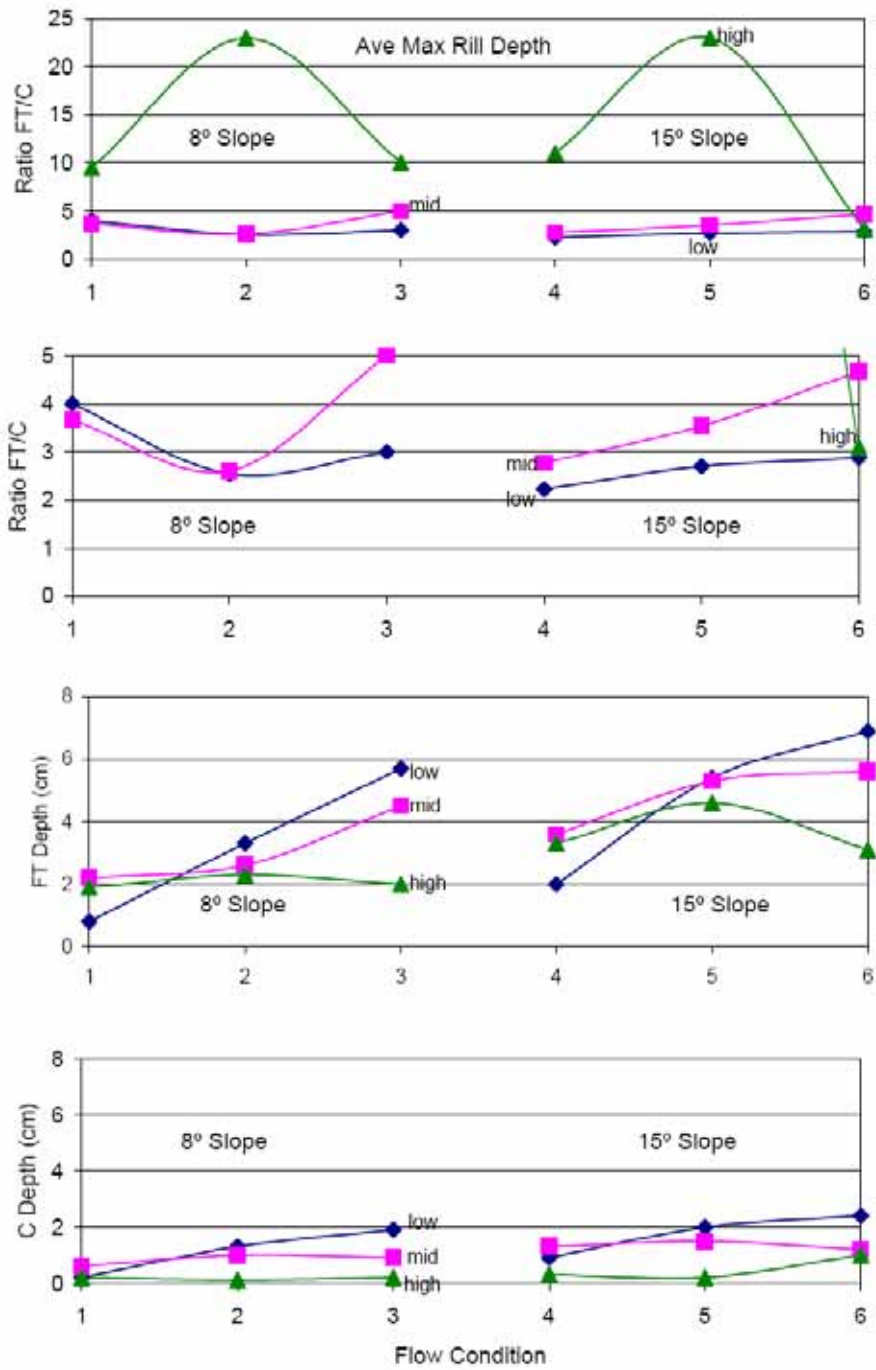


Figure 18. Average maximum FT and C rill depth and FT/C ratio with flow condition, by slope and soil moisture series. Expanded scale plot of FT/C ratio is also included.

Table 1. Experimental Conditions by Soil Moisture Series

Series	Soil Weight– mean ± stdev (kg)	Bulk Density– mean (kg/L)	Pre-test Soil Moisture mean ± stdev (% by vol)	Freezing Time mean (hr)	Post-test Soil Moisture mean ± stdev (% by vol)
Low, C	61.1 ± 0.1	1.61	17.5 ± 0.7	–	25.5 ± 2.6
Low, FT	61.1 ± 0.1	1.61	17.4 ± 0.9	51	28.2 ± 2.5
Mid, C	64.6 ± 0.4	1.71	28.6 ± 0.9	–	30.6 ± 0.6
Mid, FT	64.7 ± 0.0	1.71	28.6 ± 1.2	84	32.8 ± 0.5
High, C	74.3 ± 0.7	1.95	38.9 ± 1.1	–	37.4 ± 1.4
High, FT	74.4 ± 0.7	1.95	38.6 ± 0.5	163	37.9 ± 0.4

Table 2. Low Soil Moisture Characterization

Measurement	Control = 18.1 ± 0.9 (% by vol)		FT = 17.7 ± 1.5 (% by vol)	
	In-Rill	Out-of-Rill	In-Rill	Out-of-Rill
Penetrometer Comp Strength (kPa)	1062 ± 176	719 ± 46	1007 ± 170	598 ± 84
Vane Shear Strength (kPa)	42 ± 1.5	21 ± 2.5	39 ± 5.2	18 ± 2.3
Constant head infiltration time (s)	483	312 ± 34	283	220 ± 56
Core Measurements				
Porosity	0.41	0.43 ± 0.01	0.41	0.43 ± 0.00
% Soil Water (by volume)	17.8	17.9 ± 0.8	19.8	19.9 ± 0.7
% Saturation	43.5	41.8 ± 2.8	48.4	46.4 ± 1.7
Moist unit wt (g/cm ³)	1.77	1.72 ± 0.03	1.79	1.74 ± 0.01
Dry unit wt (g/cm ³)	1.59	1.54 ± 0.03	1.59	1.54 ± 0.00

Table 3. Mid Soil Moisture Characterization

Measurement	Control = 28.3 ± 1.7 (% by vol)		FT = 31.5 ± 2.2 (% by vol)	
	In-Rill	Out-of-Rill	In-Rill	Out-of-Rill
Penetrometer Comp Strength (kPa)	1452 ± 264	1062 ± 164	1296 ± 320	1181 ± 351
Vane Shear Strength (kPa)	27 ± 2.6	26 ± 3.4	21 ± 8.2	16 ± 8.6
Constant head infiltration time (s)	>3600 (3), 1285	257 ± 121, >3600 (1)	>3600 (2)	>3600 (3), 582
Core Measurements				
Porosity	0.35	0.38 ± 0.02	0.37	0.38 ± 0.01
% Soil Water (by volume)	29.9	29.4 ± 0.4	32.2	32.7 ± 1.4
% Saturation	85.0	77.4 ± 4.3	87.0	86.4 ± 2.4
Moist unit wt (g/cm³)	2.05	1.97 ± 0.05	2.02	2.00 ± 0.03
Dry unit wt (g/cm³)	1.75	1.67 ± 0.05	1.70	1.68 ± 0.04

Table 4. High Soil Moisture Characterization

Measurement	Control = 38.4 ± 1.2 (% by vol)		FT = 38.5 ± 1.3 (% by vol)	
	In-Rill	Out-of-Rill	In-Rill	Out-of-Rill
Penetrometer Comp Strength (kPa)	625 ± 104	572 ± 122	400	533 ± 264
Vane Shear Strength (kPa)	8 ± 2.6	8 ± 2.4	5 ± 1.2	9 ± 6.0
Constant head infiltration time (s)	>3600	>3600	>3600	>3600
Core Measurements				
Porosity	0.41	0.39 ± 0.01	0.40	0.39 ± 0.01
% Soil Water (by volume)	39.5	37.6 ± 1.3	39.6	38.5 ± 0.9
% Saturation	96.4	96.3 ± 3.3	98.5	97.9 ± 2.7
Moist unit wt (g/cm³)	2.00	2.02 ± 0.02	2.01	2.02 ± 0.03
Dry unit wt (g/cm³)	1.59	1.65 ± 0.03	1.61	1.64 ± 0.03

Table 5. Mean Groundwater Depths (cm): High Soil Moisture Series

Flow Condition	C before	FT before	C after	FT after
1	12.2	12.5	11.7	12.5
2	12.4	12.1	11.7	11.7
3	10.9	10.9	10.6	11.0
4	12.2	12.3	12.6	12.6
5	11.9	12.6	11.3	11.5
6	12.5	12.6	12.2	12.2
Mean ± stdev	12.0 ± 0.5	12.2 ± 0.6	11.7 ± 0.6	11.9 ± 0.6

Table 6. Group Averaged Sediment Load Summary

Group	FT (g/min)	C (g/min)	FT/C
Overall	37.7	12.5	3.03
Soil moisture			
Low	38.6	16.0	2.41
Mid	49.7	16.3	3.04
High	24.9	5.02	4.96
Slope			
Low	27.5	9.28	2.96
High	48.0	15.6	3.07
Flow			
Low	11.3	3.47	3.26
Mid	37.0	12.4	2.99
High	64.8	21.5	3.01

Table 7. Group Averaged 0.3L Cross-Section Norm (cm) Summary

Group	FT L_2	C L_2	FT/C L_2	FT L_{inf}	C L_{inf}	FT/C L_{inf}
Overall	1.81	0.64	2.81	3.40	1.21	2.81
Soil Moisture						
Low	1.48	0.80	1.87	3.13	1.85	1.69
Mid	2.48	0.83	2.97	4.12	1.27	3.25
High	1.47	0.30	4.89	2.95	0.52	5.71
Slope						
Low	1.46	0.63	2.31	2.63	1.10	2.39
High	2.16	0.65	3.31	4.17	1.32	3.15
Flow						
Low	0.83	0.23	3.54	1.95	0.47	4.18
Mid	1.98	0.71	2.79	3.80	1.52	2.51
High	2.62	0.98	2.66	4.45	1.65	2.70

Table 8. Group Averaged 0.7L Cross-Section Norm (cm) Summary

Group	FT L_2	C L_2	FT/C L_2	FT L_{inf}	C L_{inf}	FT/C L_{inf}
Overall	2.33	0.47	4.94	4.15	0.91	4.56
Soil Moisture						
Low	2.53	0.35	7.24	5.18	0.98	5.27
Mid	2.78	0.83	3.34	4.35	1.25	3.48
High	1.68	0.23	7.21	2.92	0.50	5.83
Slope						
Low	2.04	0.44	4.64	3.48	0.83	4.17
High	2.62	0.50	5.21	4.82	0.99	4.88
Flow						
Low	1.07	0.35	3.05	2.42	0.65	3.72
Mid	2.38	0.55	4.37	4.40	1.18	3.72
High	3.55	0.52	6.81	5.63	0.90	6.26

Table 9. Group Averaged Maximum Rill Width and Depth Summary

Group	FT width (cm)	C width (cm)	FT/C width	FT depth (cm)	C depth (cm)	FT/C depth
Overall	4.62	3.87	1.19	3.62	0.96	3.79
Soil Moisture						
Low	4.17	4.33	0.96	4.02	1.45	2.77
Mid	5.77	5.42	1.07	3.97	1.08	3.66
High	3.93	1.87	2.11	2.87	0.33	8.60
Slope						
Low	4.16	3.72	1.12	2.81	0.71	3.95
High	5.09	4.02	1.26	4.42	1.20	3.69
Flow						
Low	3.23	2.92	1.11	2.30	0.58	3.94
Mid	4.65	3.78	1.23	3.92	1.02	3.85
High	5.98	4.92	1.22	4.63	1.27	3.66

Table 10. Approximately Replicated Experimental Conditions

Experiment	Soil Weight (kg)		Soil Moisture (% by vol)		Average Flow (L/min)		Duration (min)	Ending WS Slope	
	FT	C	FT	C	FT	C		FT	C
Low Moisture 6	61.1	61.1	18.9	18.7	2.07	2.12	45	0.156	0.278
Replicate	57.9	57.9	15.0	15.4	2.54	2.54	36	0.195	0.260
High Moisture 4	74.9	74.9	38.3	38.1	0.393	0.377	63.5	0.291	0.300
Replicate	74.7	74.7	33.7	35.9	0.405	0.408	83	0.280	0.289
High Moisture 4–Light	61.1	61.1	38.4	36.3	0.419	0.409	63	0.245	0.259
Replicate	61.1	61.1	37.2	35.1	0.403	0.403	64	0.250	0.262

Table 11. Differences in Results of Replicated Experiments

Quantity	Low Moisture 6				High Moisture 4				High Moisture 4–Light			
	ΔFT	ΔC	$\Delta FT/FT$	$\Delta C/C$	ΔFT	ΔC	$\Delta FT/FT$	$\Delta C/C$	ΔFT	ΔC	$\Delta FT/FT$	$\Delta C/C$
Mean Concentration	1.1	4.9	0.03	0.33	31.3	1.9	0.51	0.36	2.9	1.2	0.08	0.56
TimeWt Concentration	1.8	7.8	0.05	0.57	20.6	1.6	0.48	0.45	1.6	0.9	0.06	0.63
Median Concentration	2.8	3.4	0.06	0.26	27.9	1.4	0.55	0.42	0.3	1.3	0.01	0.72
Max Concentration	25.6	1.8	0.42	0.06	125	3.9	0.66	0.25	21.1	2.3	0.29	0.42
Sediment Load	23.1	25.6	0.28	0.88	7.8	0.5	0.47	0.40	1.0	0.4	0.10	0.64
Total Sediment Trans	0.1	0.7	0.03	0.50	0.3	0.0	0.31	0.22	0.1	0.0	0.08	0.63
L_2 at 0.3L	0.5	4.7	0.16	9.40	0.4	0.2	0.36	0.67	0.1	0.0	0.20	1.00
L_{inf} at 0.3L	0.3	5.4	0.05	3.86	1.0	0.3	0.37	0.50	0.5	0.1	0.33	1.00
L_2 at 0.7L	3.2	3.0	1.07	30.0	0.2	0.1	0.17	0.50	0.3	0.1	0.50	1.00
L_{inf} at 0.7L	1.7	3.9	0.25	9.75	0.8	0.1	0.30	0.25	1.5	0.3	0.65	1.00
Avg Max Rill Width	2.8	1.1	0.58	0.17	1.0	0.5	0.29	0.36	0.3	0.9	0.12	0.69
Avg Max Rill Depth	1.0	1.3	0.14	0.54	0.2	0.1	0.06	0.33	0.2	0.3	0.10	0.90

Table 12. Low Moisture 2–Dry: Comparison of FT and C at Very Low Moisture

Quantity	<i>FT</i>	<i>C</i>	<i>FT / C</i>	$ FT - C $	$\frac{ FT - C }{FT}$
Soil Weight (kg)	52.2	52.2	1.000	0.0	0.0
Soil Moisture (% by vol)	4.4	5.2	0.846	0.8	0.18
Average Flow (L/min)	1.07	1.07	1.000	0.0	0.0
Duration (min)	65				
Mean Concentration (g/L)	21.0	19.1	1.099	1.9	0.09
Time Wt Concentration (g/L)	21.4	21.0	1.019	0.4	0.02
Median Concentration (g/L)	19.1	18.2	1.049	0.9	0.05
Maximum Concentration (g/L)	42.1	34.1	1.235	8.0	0.19
Sediment Load (g/min)	22.9	22.5	1.018	0.4	0.02
Total Sediment Transport (g)	170	161	1.056	9	0.05
L_2 at 0.3L (cm)	2.0	1.8	1.111	0.2	0.10
L_{inf} at 0.3L (cm)	3.4	2.7	1.259	0.7	0.21
L_2 at 0.7L (cm)	2.6	2.2	1.182	0.4	0.15
L_{inf} at 0.7L (cm)	4.3	4.2	1.024	0.1	0.02
Avg Maximum Rill Width (cm)	4.7	5.2	0.904	0.5	0.11
Avg Maximum Rill Depth (cm)	3.7	3.6	1.028	0.1	0.03

